World Journal of Advanced Research and Reviews
eISSN: 2581-9615 CODEN (USA): WJARAI
Cross Ref DOI: 10.30574/wjarr
Journal homepage: https://wjarr.com/

(RESEARCH ARTICLE)

Check for updates

Chemical thermodynamics of biomass, cellulose, and cellulose derivatives: A review

Michael Ioelovich *

Designer Energy Ltd, 2 Bergman Str., Rehovot 7670504, Israel.

World Journal of Advanced Research and Reviews, 2024, 24(01), 1295–1338

Publication history: Received on 03 September 2024; revised on 13 October 2024; accepted on 15 October 2024

Article DOI: https://doi.org/10.30574/wjarr.2024.24.1.3145

Abstract

This article provides a review of the research on the chemical thermodynamics and thermochemistry of biomass, cellulose, and its derivatives such as ethers, esters, and oxycelluloses. For diverse biomass types, gross and net heating values were studied. It has been established that these energetical characteristics of biomass can be calculated using a superposition of the energetical characteristics of the main components of biomass such as cellulose, hemicelluloses, lignin, lipids, proteins, etc. The pelletization of biomass improves its fuel performance. It was shown that, if the ultimate goal is to generate the maximum amount of thermal energy, then it is more profitable to directly burn the initial biomass in the form of pellets than to burn the amount of solid or liquid biofuel that can be extracted from this biomass.

After the cellulose study, the direct and exact thermochemical method for determining the crystallinity degree of this biopolymer was proposed. In addition, the standard combustion and formation enthalpies of various cellulose samples were studied. As a result, the thermodynamic characteristics of four crystalline allomorphs of cellulose, CI, CII, CIII, and CIV, were obtained and their thermodynamic stability was evaluated. The thermochemistry of enzymatic hydrolysis of cellulose was studied. In addition. The thermodynamical characteristics of various cellulose derivatives were determined, and the thermochemistry of the reactions of cellulose alkalization, etherification, esterification, and oxidation was studied.

Keywords: Biomass; Cellulose; Cellulose derivatives; Thermodynamics; Thermochemistry

1. Introduction

Chemical thermodynamics is one of the parts of physical chemistry the main purposes of which are to determine the thermodynamic functions, study the transformation of various forms of energy during chemical reactions and phase transitions, predict the feasibility and direction of chemical processes, as well as examine the ability of chemical systems to perform useful work [1]. A section of chemical thermodynamics is thermochemistry, which studies the thermal effects of chemical reactions and physicochemical processes.

Chemical thermodynamics operates with thermodynamic functions [1]. At a constant pressure, these functions are enthalpy (H), entropy (S), and Gibbs potential (G). The thermodynamic tables contain the so-called standard formation enthalpies ($\Delta_f H^o$) and entropies (S^o) of various substances, calculated for standard conditions, at temperature T^o=298.15 K and pressure P^o=0.1 MPa. If the standard formation enthalpy of an organic substance $C_xH_yO_z$ is unknown, it can be calculated from the experimentally determined combustion enthalpy ($\Delta_c H^o$) of this substance at standard conditions. The combustion process of the substance can be described, as follows:

$$C_xH_yO_z + (x + 0.25y - 0.5z)\ O_2 \rightarrow x\ CO_2 + 0.5y\ H_2O + \Delta_c H^o(C_xH_yO_z) \quad \text{.....(1)}$$

Then, the standard formation enthalpy of this substance can be calculated by the following equation:

* Corresponding author: Michael Ioelovich

$$\Delta_f H^o(C_xH_yO_z) = x\,\Delta_f H^o(CO_2, g) + 0.5y\,\Delta_f H^o(H_2O, l) - \Delta_c H^o(C_xH_yO_z) \quad \text{(2)}$$

where $\Delta_f H^o(CO_2, g) = -393.51$ kJ/mol and $\Delta_f H^o(H_2O, l) = -285.83$ kJ/mol are standard enthalpies of the formation of carbon dioxide and liquid water, respectively.

The thermodynamics of a chemical reaction at standard conditions can be considered in more detail. Let there be a reaction between reagents R_1 and R_2 with the formation of reaction product RP:

$$R_1 + R_2 \rightarrow RP \quad \text{(3)}$$

The change in the standard thermodynamic Gibbs potential of a reaction can be generally expressed by the equation:

$$\Delta_r G^o(RP) = \Delta_r H^o(RP) - T^o\Delta_r S^o(RP) \quad \text{(4)}$$

where

$$\Delta_r H^o(RP) = \Delta_f H^o(RP) - \Delta_f H^o(R_1) - \Delta_f H^o(R_2) \quad \text{(5)}$$

and

$$\Delta_r S^o(RP) = S^o(RP) - S^o(R_1) - S^o(R_2) \quad \text{(6)}$$

These standard thermodynamic characteristics of substances R_1, R_2, and RP can be found in reference books or calculated from experiments.

If $\Delta_r G^o(RP) < 0$, this reaction is feasible, but if $\Delta_r G^o(RP) > 0$, then such a reaction cannot be implemented.

Suppose it is necessary to find the values of thermodynamic characteristics at other temperatures. In that case, you can use reference data on the temperature dependence of the specific heat capacity (C_p) of a substance. The formation enthalpy of a substance at temperature T can be found using the equation:

$$\Delta_f H\,(T) = \Delta_f H^o + \int_{298.15}^{T} Cp\,dT \quad \text{(7)}$$

The entropy of a substance at temperature T is calculated as follows:

$$S(T) = S^o + \int_{298.15}^{T} \left(\frac{Cp}{T}\right) dT \quad \text{(8)}$$

The thermodynamic functions of the reaction $R_1 + R_2 \rightarrow RP$ at temperature T can be calculated. using the following equations:

$$\Delta_r H(RP) = \Delta_f H(RP) - \Delta_f H(R_1) - \Delta_f H(R_2) \quad \text{(9)}$$

$$\Delta_r S(RP) = S(RP) - S(R_1) - S(R_2) \quad \text{(10)}$$

Further, the change in the thermodynamic Gibbs potential of the reaction at temperature T is calculated:

$$\Delta_r G(RP) = \Delta_r H(RP) - T\Delta_r S(RP) \quad \text{(11)}$$

If $\Delta_r G(RP) < 0$, this reaction can proceed, but if $\Delta_r G(RP) > 0$, then such a reaction is impossible.

There are many applications of chemical thermodynamics to various substances (inorganic, organic, monomeric, polymeric, synthetic, natural, etc.) and diverse reaction classes (synthesis, decomposition, substitution, exchange, oxidation, reduction, etc.). Currently, due to the lack of fossil fuels and the harm their use causes to the environment, much attention is paid to the use of renewable natural resources such as plant biomass.

The existence and further development of the present civilization require expanded consumption of energy, chemicals, and materials. Nowadays, the main energy sources are fossil fuels, namely coal, petroleum, and natural gas [2]. However, the increased use of fossil fuels is causing acute environmental problems, since the combustion of such fuels is

accompanied by the emission of carbon dioxide and water vapor, triggering the greenhouse effect and global warming. An additional problem is that fossil resources are not reproduced in nature. Therefore, their reserves are exhausted and run down in an essentially permanent manner [3].

To eliminate the imbalance in the fossil sources, an increased utilization of alternative sources of energy and raw materials is required. Considerable attention in recent years has been given to plant biomass, which in contrast to fossil sources is continuously renewed in nature. The total resources of plant biomass reach 1.5 trillion tons [4]. Currently implemented technologies for the production of liquid biofuels are based on the transformation of carbohydrates into bioethanol and vegetable oils into biodiesel fuel. The main sources of these carbohydrates are juices of sugarcane, sugar beet, and sweet sorghum, as well as starches of corn, wheat, potatoes, and some other agricultural plants. Since these carbohydrates and vegetable oils are required in the food industry, their use for the production of biofuels is limited. Moreover, further expansion of the production to a higher volume of bioethanol and/or biodiesel will cause a shortage of land areas, exhaustion of the soil, excessive consumption of water and energy, deficits of food and feed products, and increase their prices [5].

An alternative way to obtain biofuels without competing with the food and feed industry is the use of inedible biomass, which is an abundant, renewable, and inexpensive plant material. This biomass type involves energy crops (e.g., miscanthus, switchgrass, Bermuda grass, *etc*.), forest residues (e.g., sawdust, twigs, shrubs, *etc*.), residues of agricultural plants (*e.g*. stalks, husks, cobs, *etc*.), residues of textile, pulp, and paper, municipal paper waste, etc. Moreover, huge amounts of algae can be used as appropriate feedstock for the production of bioenergy or chemicals. The total resources of inedible biomass accumulated annually are estimated at 10 billion tons, the combustion of which can generate about 150 EJ of bio-energy.

The biomass of any plant is formed in nature from carbon dioxide and water by photosynthesis-absorbing solar energy [6]. Thus, a plant biomass is an accumulator of solar energy captured during photosynthesis. When the plant biomass is burned, this results in the release of accumulated solar energy, along with water and carbon dioxide. Therefore, biomass is considered a CO_2-neutral renewable natural source [7]. The incomplete combustion of biomass over an open fire leads to the formation of harmful aerosol microparticles. However, when the biomass is burned in combustion chambers equipped with special smoke filters, these microparticles are captured, which prevents air pollution [8].

An important component of biomass is cellulose, the most abundant organic matter on Earth. The total resources of cellulose in nature attain half a trillion tons and are constantly renewed in nature as a result of photo-biosynthesis [9]. Cellulose is present in all plants and algae; tunicate cellulose is also known, which forms the shell of certain marine creatures; in addition, cellulose is synthesized by some microorganisms, e.g. *Gluconacetobacter xylinus*. The main sources of cellulose are plants. The content of cellulose in herbaceous plants is 30-40%, in woods 45-50%, in bast plants (flax, ramie, etc.) 60-70%, and in cotton fibers upwards of 90% [10].

The main commercial sources of cellulose are wood and to a lesser extent - cotton. To isolate the cellulose, the feedstocks are boiled in boilers under pressure in the presence of caustic soda (Soda process), a mixture of sodium hydroxide with sodium sulfide (Kraft process) or sulfurous acid and salts thereof (Sulfite process) [11]. Organosolv, oxidative, and some other delignification methods are also used, but on a lower scale. As a result, lignin and hemicelluloses are removed, while cellulose is separated, washed, and dried. The production volume of wood cellulose in the world is huge and reaches 250-300 million tons per year. Production of cotton cellulose is smaller, 20-25 million tons per year. The main part of the cotton fibers is intended for the textile industry, and only short fibers (linter) and cotton wastes (nap) are used to produce chemical grade cellulose, special paper kinds, microcrystalline cellulose, and cellulose derivatives.

Cellulose is an inexhaustible natural source of raw materials used for the production of textiles, paper, cardboard, fibers, films, fillers, binders, glues, explosives, drugs, and other valuable materials and substances. Cellulose is a linear, stereoregular, semicrystalline polysaccharide composed of repeating anhydroglucose units (AGUs) having a “chair” conformation and linked by chemical β-1,4-glycosidic chemical bonds. Macromolecules of natural cellulose of various origins may include 2,000 to 30,000 AGUs. In the process of cellulose isolation from plant raw materials and modification of this biopolymer, partial depolymerization of its macromolecules may occur.

Each anhydroglucose unit of cellulose contains three hydroxyl functional groups: one primary and two secondary groups. The hydroxyl groups impart to cellulose materials an increased hydrophilicity and water absorption ability. Besides, owing to hydroxyl groups, cellulose can form diverse derivatives, such as ethers and esters, carbonyl, carboxyl, and other derivatives. Due to the presence in non-crystalline domains of cellulose of labile glycosidic (semi-acetal) chemical bonds, this polysaccharide is depolymerized under the effect of oxidants, acids, and cellulolytic enzymes [12].

The linear macromolecules joined by hydrogen bonds form the supramolecular structure of this biopolymer, which consists of elementary nanofibrils and their bundles called microfibrils. Moreover, each nano-scale fibril is built of ordered nanocrystallites and low-ordered non-crystalline nanodomains. The nanocrystallites having three-dimensional order are strong and inaccessible structural elements. However, the low-ordered non-crystalline nanodomains having twisted and curved segments are weak and accessible places of the fibrils. Molecular chains of cellulose pass through several crystallites and non-crystalline domains linking them by strong chemical bonds. Thereby, cleavage of glycosidic bonds at the hydrolysis occurs mainly in non-crystalline domains of cellulose nanofibrils that facilitate the release of the individual crystallites. The formed crystalline fragments have a level-off degree of polymerization (LODP) from 100 to 300 approximately corresponding to an average degree of polymerization of individual nanocrystallites [13].

The supramolecular structure of cellulose has been studied since the 19th century when Carl von Nägeli proposed the idea that natural cellulose contains crystalline micelles – small crystallites [14, 15]. Only 70 years later this idea was confirmed by X-ray diffraction. As a result, the first model of the monoclinic unit cell for the crystalline structure of native cellulose CI was developed by Mayer and Mish [16]. The model of Mayer and Mish with antiparallel arrangement of chains existed for 30 years, after which it was replaced by a more accurate model with parallel arrangement of cellulose chains within crystallites [17]. Later it was discovered that in addition to the crystalline structure of native cellulose CI, there are also other crystalline allomorphs, CII, CIII, and CIV [18].

Nano-scale crystallites of various types along with non-crystalline domains are integral constituents of long and thin filaments called elementary fibrils. Thus, a two-phase cellulose model containing crystalline and non-crystalline domains is currently used to describe the structural organization of cellulose [19]. Further investigations revealed the presence also of paracrystalline fraction, which must be taken into consideration when developing an improved model of the cellulose structure [20, 21].

Due to the difficult molecular and supramolecular structure cellulose is an excellent object of thermodynamic investigations that can include:

- Study interaction enthalpies of cellulose with various liquid media for application in structural analysis of this biopolymer
- Determination of standard thermodynamic functions of cellulose samples of various origins
- Determination of standard thermodynamic functions of cellulose crystallites having different allomorphs, CI, CII, CIII, and CIV, and amorphous cellulose
- Study thermodynamics of phase transitions in cellulose
- The effect of nanosized cellulose crystallites on the specificity of their phase transition
- Determination of standard thermodynamic functions of various cellulose derivatives having different degrees of substitution
- Study of chemical thermodynamics of cellulose derivatization – reactions of esterification, etherification, oxidation, etc.
- Etc.

2. Material and methods

The various biomass samples were studied, the chemical composition of which was found using standard methods of chemical analysis [22].

The studied cellulose samples were:

- Pure chemical-grade cotton cellulose (CC) of Hercules, Inc. (Wilmington, DE, USA)
- Microcrystalline cellulose (MCC) prepared by treatment of CC with boiling 2.5 M HCl for 1 h at the acid-to-CC ratio of 20, followed by washing and drying
- Microcrystalline cellulose Avicel PH-101 (MCCA) of FMC
- Mercerized CC (CCM) prepared by treatment of CC with 6 M NaOH for 1 h at room temperature and alkali-to-CC ratio of 20, followed by washing and drying
- Ball-milled CC for 8 h (BC)
- Cotton cellulose treated with liquid ammonia (CCA) for 3 h and dried at room temperature
- CCA treated with hot glycerol at 533 K (CCAG) for 1 h, followed by washing and drying
- Bleached high-pure sulfite spruce pulp (SP) of Weyerhaeuser Co. (Seattle, WA, USA)

- Bleached Kraft pine chemical pulp (KP) of Weyerhaeuser, further refined by treatment with 2 M NaOH for 1 h at room temperature and the alkali-to-pulp ratio of 20, followed by washing and drying
- KP treated with liquid ammonia (CCA) for 3 h and dried at room temperature
- KPA treated with hot glycerol at 533 K (KPAG) for 1 h, followed by washing and drying
- Mercerized KP pulp (KPM) prepared by treatment of KP with 6 M NaOH for 1 h at room temperature and the alkali-to-pulp ratio of 20, followed by washing and drying
- Viscose rayon fibers (VF) of Rayonier, Inc. (Wildlight, FL, USA)
- Some other cellulose samples

The main characteristics of the cellulose samples are shown in Table 1.

Table 1 Characteristics of cellulose samples

Sample	Allomorph	Cellulose, %	Ash, %	DP
MCCA	CI	>99	<0.01	220
MCC	CI	>99	<0.01	170
CC	CI	>99	<0.01	2700
KP	CI	>99	<0.02	1200
SP	CI	>99	<0.02	1100
BC	CI	>98	<0.05	640
CCM	CII	>99	<0.01	2100
KPM	CII	>99	<0.02	1000
VF	CII	>99	<0.02	350
CCA	CIII	>99	<0.01	2700
KPA	CIII	>99	<0.02	1200
CCAG	CIV	>98	<0.02	430
KPAG	CIV	>97	<0.02	380

2.1. Standard Combustion Enthalpy

Combustion of the dry samples was carried out in a stainless-steel calorimetric bomb having a volume of 0.320 dm^3 at an oxygen pressure of 3.05 MPa with 1.00 cm^3 of deionized water added to the bomb [23]. The combustion measurements were carried out by an isothermal water calorimeter at 298.15 K with an accuracy of ±0.001 K. To adjust the enthalpy of combustion (Δ_cH) to standard conditions the Washburn correction, as well as the correction for the change in the number of moles of gases before and after combustion was introduced. For each sample, five experiments were performed to calculate the reliable value of combustion enthalpy and standard deviation.

2.2. Specific Heat Capacity and Entropy

Specific heat capacities (C_p) of dry samples were measured in the temperature range of 80-340 K using an adiabatic vacuum calorimeter. Below 80 K, C_p values were estimated by the method of Kelly, et al. [24]. For each sample, four experiments were performed to calculate the reliable C_p value and standard deviation.

The entropy values of the samples at temperature T were calculated, as follows:

$$S(T) = \int_0^T \left(\frac{Cp}{T}\right) dT \quad \text{..... (12)}$$

If T is the standard temperature T^o = 298.15 K, then the calculated result is the standard entropy S^o of the sample.

2.3. Standard Enthalpy of Interaction of Samples with Liquid Media ($\Delta_i H^o$)

$\Delta_i H^o$-values, including the standard enthalpies of samples wetting with water ($\Delta_w H^o$), were studied at 298.15 K using a TAM Precision Solution Calorimeter [25]. A small sample was used in the form of pieces, fibers, or powders. Before starting the experiments, the air-dry sample was put into a special glass ampoule and dried in a vacuum at 378 K to a constant weight. The glass ampoule containing the dry sample was sealed and introduced into the calorimetric cell filled with a liquid. The calorimeter was thermostated at 298.15 K to achieve an equilibrium state. Thereafter, the sealed ampoule with the dry sample was broken to ensure the contact of the sample with a liquid. The released heat effect ($\Delta_i H^o$ or $\Delta_w H^o$) was measured with accuracy ±0.01 J. Three of the same samples were tested to calculate an average enthalpy value and standard deviation.

2.4. Wide Angle X-ray Scattering (WAXS)

In the WAXS method, the experiments were carried out on a Rigaku-Ultima Plus diffractometer (CuKα-radiation, λ = 0.15418 nm) in the φ =2Θ-angle range from 5 to 50° using a reflection mode [9]. Collimation included a system consisting of vertical slits and Soller slits. The procedure of 0.02^0 step-by-step scanning was used to determine the exact position of the peaks. The tested specimens in the shape of tablets with a diameter of 16 mm and a thickness of 2 mm were prepared from washed and dried samples by pressing at a pressure of 50 MPa. Three diffractograms were recorded for each cellulose sample to calculate the average CrI value and its standard deviation.

2.5. Specific Surface Area

The sorption of nitrogen by samples was measured at 77K using Sorptometer QBET-NV1A of Porous Material Inc. The sorption of n-hexane vapor was carried out at 298 K on a *vacuum Mac-Ben apparatus* having helical spring quartz scales. Before starting the experiments, the samples were dried at 378 K to constant weight and degassed under vacuum. Three of the same samples were tested to calculate an average sorption value and standard deviation that was in the range CD = ± 0.002 g/g. The specific surface area (A_{sp}) of the samples was measured from sorption isotherms by the BET method [26]. Using this method, the monomolecular adsorption value, a_m (g/g), was found, after which the value of A_{sp} (m^2/g) was calculated. In the case of low-temperature N_2 sorption A_{sp} (N_2) = 3034.3 a_m, and for sorption of n-hexane vapor A_{sp} (H)= 2086.5 a_m

3. Results and discussion

3.1. Thermochemistry of Plant Biomass

To assess the energy potential of biomass as a solid biofuel, it is necessary to determine its higher (gross) and lower (net) heating values. The higher heating value (HHV) is equivalent to the standard enthalpy of combustion, which is the amount of thermal energy released during the complete combustion of fuel at a standard temperature in conditions providing condensation of water vapor. The lower heating value (LHV) is the amount of thermal energy released during the complete combustion of fuel at a standard temperature in such conditions when the condensation of water vapor is excluded. Thus, HHV is greater than LHV by the amount of condensation heat of water vapor formed during the complete combustion of the fuel.

Any biomass contains several main components such as cellulose, hemicellulose, lignin, lipids, and inorganic substances that produce ash when calcined. In addition to the main components, some biomasses may contain starch, pectin, proteins, pigments, etc. If the original biomass is subjected to physicochemical or biological treatment, its chemical composition may change. Since biomasses have different chemical compositions, their fuel properties will also be different, as can be seen in Table 2.

Table 2 Higher (Q) and lover heating value (q) of dry biomass samples*

Biomass	Holo, %	Lignin, %	Lipids, %	Prot., %	Ash, %	-Q, MJ/kg	-q, MJ/kg
Used printing paper	69	1	1	0	29	12.5	11.4
Used newspaper	59	22	1	0	18	16.1	15.0
Rice straw	72	8	3	1	16	15.7	14.4
Rice husk	59	20	2	2	17	16.5	15.2
Corn stover	70	19	3	2	6	18.1	17.0

Wheat straw	74	16	2	2	6	18.2	17.1
Switchgrass	72	18	3	2	5	18.3	17.0
Miscanthus	73	19	2	2	4	18.6	17.3
Used cardboard	81	11	1	0	7	17.1	15.0
Cotton linter	98	0	1	0	1	17.8	16.0
Cotton stalks	81	17	1	0	1	17.7	15.8
Waste of textile	97	0	2	0	1	18.0	16.2
Bagasse	70	20	3	2	5	19.1	17.7
Softwood sawdust	69	27	2	0	2	19.8	18.6
Olive pomace	56	33	7	2	2	22.3	20.0
Fallen olives	37	22	35	3	3	26.0	24.3

*Holo denotes Holocellulose, which is the sum of cellulose, hemicelluloses, and other polysaccharides. Prot. denotes Proteins. The minus sign on Q & q denotes the exothermic process

A detailed study of the effect of some components on the heating values showed that lignin and lipids contribute to the increase of thermal energy of the biomass, while inorganic components (ash) reduce this energy. High-lignified and lipid-rich biomass types such as fallen olives have an increased thermal energy. Vice versa, a biomass containing a small amount of lignin and lipids, but a large amount of ash and moisture has a low energetic potential. To improve the fuel performance of biomass, it must have reduced moisture and ash content, as well as an increased density. Therefore, before burning the biomass should be dried, demineralized, and densified into fuel pellets [8].

Table 3 Average higher and lower heating values of biomass components [27]

Component	-Qi, MJ/kg	-qi, MJ/kg
Holo*	17.5	16.2
Lignin	26.0	24.5
Lipids	38.6	36.2
Proteins	22.0	20.0
Ash	0	0

*Holo denotes Holocellulose, which is the sum of cellulose and hemicelluloses

There are several methods for calculating the energy potential of biomass. The first of them is based on the additivity rule:

$$Q = 0.01 \sum C_i Q_i \quad \text{..... (13)}$$

$$q = 0.01 \sum C_i q_i \quad \text{..... (14)}$$

where C_i is the percentage content of components (see e.g., Table 2); Q_i and q_i are HHV and LHV of the component of the biomass (Table 3).

Table 4 Higher and lower heating values of biomass samples calculated by eq. (13) and (14)

Biomass	$-Q_c$, MJ/kg	$-q_c$, MJ/kg
Softwood sawdust	19.9	18.5
Bagasse	19.0	17.7
Rice husk	16.7	15.5

The second method is based on elementary analysis and determination of the percentage content of carbon (C, %), hydrogen (H, %), sulfur (S, %), and nitrogen (N, %) in the biomass. Then the higher and lower heating values of the biomass can be calculated as follows [28]:

$$Q\ (MJ/kg) = -(0.344\ C + 1.217\ H + 0.105\ S - 0.106\ O - 0.015\ N) \quad (15)$$

$$q\ (MJ/kg) = -(0.344\ C + 1\ H + 0.105\ S - 0.106\ O - 0.015\ N) \quad (16)$$

For example, the elemental analysis shows the following results (Table 5):

Table 5 Elemental compositions of biomass samples and calculated heating values

Biomass	C, %	H, %	O, %	S, %	N, %	$-Q_c$, MJ/kg	$-q_c$, MJ/kg
Softwood sawdust	50	6.2	44	0	1	20.0	18.7
Bagasse	48	6.0	42	0	1	19.3	17.9
Rice husk	39	6.8	50	1	3	16.4	15.0

The comparison showed that the calculated heating values (Q_c and q_c) differ from the experimental ones (Q and q) by no more than 3%.

It is known that biomass can also be used as a feedstock for the production of char through the pyrolysis process and ethanol through enzymatic hydrolysis. However, analysis shows that the amount of thermal energy of solid (char) and liquid (ethanol) biofuels that can be extracted from 1 t of the biomass is significantly lower than the energetic potential of 1 t of the starting biomass [2, 8]. For example, the amount of biochar (BC) that can be obtained from 1 t of switchgrass (SG) after pyrolysis is about 340 kg, the gross energy of which is E (BC) = -10.2 GJ. Since the gross energetic potential of 1 t of initial SG is Q (SG) = -18.3 GJ, the energy yield of biochar from this biomass is 56%. It was also shown that the volume of bioethanol that can be obtained from 1 t of SG after pretreatment and enzymatic hydrolysis steps is 206 L having a gross energy of E (BE) = -5 GJ [8]. Thus, the yield of gross energy of this liquid biofuel from SG biomass is 27% only.

Thus, if the ultimate goal is to generate the maximum amount of thermal energy, then it is more profitable to directly burn the initial biomass in the form of pellets than to burn the amount of solid or liquid biofuel that can be extracted from this biomass.

3.2. Thermochemical Method to Determine the Crystallinity and Amorphicity Degree of Cellulose Materials

A characteristic feature of cellulose is crystallinity, which depends on the origin of cellulose, and the treatment method and conditions of processing this biopolymer [29]. It is known that the crystallinity of pure cotton cellulose is higher than that of cellulose extracted from wood or grass [9]. Acid hydrolysis of cellulose promotes an increase in crystallinity of this biopolymer [20], while the ball-grinding [30], and treatment with liquid ammonia, primary amines, diamines, some solvents, and concentrated solutions of alkalis [31] lead to a decrease in cellulose crystallinity.

However, in the structural analysis of cellulose samples, a problem arises due to the lack of an accurate method for determining the degree of crystallinity. There are only approximate indices of cellulose crystallinity, which can be estimated by such methods as wide-angle X-ray scattering (WAXS), solid-state ^{13}C-NMR, FTIR, Raman spectroscopy, as well as by physicochemical (e.g., sorption iodine), chemical (e.g., hydrolysis with boiling 2.5 M HCl) methods, etc. [20, 21, 32-36].

Unfortunately, different methods give different values of the crystallinity index (CrI) for the same cellulose sample; therefore, it is not clear which value of CrI should be preferred. Even applying the same method, e.g., WAXS, also gave different CrI values for the same sample if different measurement techniques were used to separate X-ray scattering from the crystalline and amorphous domains. So, the study of microcrystalline cellulose Avicel PH-101 showed that the measuring of peak heights gave CrI 0.80–0.93, deconvolution of the peaks gave CrI 0.55–0.61, subtraction of amorphous scattering gave CrI 0.60–0.78, Ruland's technique gave CrI 0.55–0.61, the technique of Jayme–Knolle gave CrI about 0.69, and the technique of Hermans–Weidinger gave CrI ranging from 0.63 to 0.82 [32-34].

Moreover, if one technique of the same method for the same sample (e.g., Avicel PH-101) is used, then the CrI value obtained by different researchers turns out to be poorly reproducible [34]. There are several main reasons for the large discrepancies in the values of the crystallinity indices when they are evaluated by different methods or by different measurement techniques of the same method. Firstly, it is due to the application of different calculating equations, mathematical functions, and software to calculate CrI. Secondly, it is due to the different experimental conditions of different methods. Thirdly, it is due to the use of inadequate structural models to evaluate the crystallinity of real cellulose samples. In addition, there are no standard protocols for preparing cellulose samples for the determination of their crystallinity. In particular, the value of the X-ray crystallinity index is affected by the type of crystalline allomorph, the size of crystallites, the distortions, and the texture of the sample. Thus, it is not possible to conclude which of the currently used methods and/or measurement techniques of cellulose crystallinity is the most appropriate. Therefore, it is advisable to develop a new method operating on other principles, namely the thermochemical method based on the measurement of the wetting enthalpy of various cellulose samples.

During isolation, purification, modification, and application, cellulose undergoes the action of various liquids. As a result of interaction, cellulose sorbs a liquid that is accompanied by the heat effect of interaction and changes in structure and properties of this biopolymer depending on the nature of the liquid [37, 38]. It was found that for the same cellulose sample, the absolute value of enthalpy of interaction depends on the nature of the liquid, and increases in the following order of the liquids [38]:

Hydrocarbons < Higher alcohols < Lower alcohols < Water < Polar organic solvents

The study reveals that in the case of non- and low-polar liquids (e.g. hexane, acetone, acetic acid, higher alcohols, etc.) the heat of interaction of different cellulose samples with these liquids is relatively small and depends mainly on the specific surface area of the samples. This evidences that the interaction of non- or low-polar liquids occurs on the accessible surface of cellulose. However, when the cellulose samples interact with highly polar liquids such as water, DMF, DMS, amines, and some others, the obtained interaction heat is directly proportional to the content of non-crystalline domains (NCD); thereby the interaction of these liquids is carried out with polar groups in NCD of cellulose by the absorption mechanism.

Water is the most common medium used in the technology of cellulose materials. Being a typical hydrophilic biopolymer, cellulose interacts with water during cellulose isolation from natural materials; during wetting, cleaning, and washing of cellulose; during papermaking processes; at cellulose activation to chemical modification, and during some other processes. Various methods can be used to study the interaction of cellulose with water, the most important of which is the study of the thermal effect of the interaction of cellulose samples with water, i.e., the wetting enthalpy, that can be used to determine crystallinity and amorphicity degrees of cellulose samples.

From the structural studies of the cellulose samples, it follows that the X-ray diffraction pattern of the cotton cellulose (CC) is typical of natural cellulose containing a crystalline allomorph of CI with characteristic peaks at 2Θ angles of 14.9, 16.5, 22.7, and 34.7° due to X-ray diffraction from planes of the CI-crystalline lattice with Miller indices of (1$\bar{1}$0), (110), (200), and (004), respectively (Figure 1, X-pattern 1).

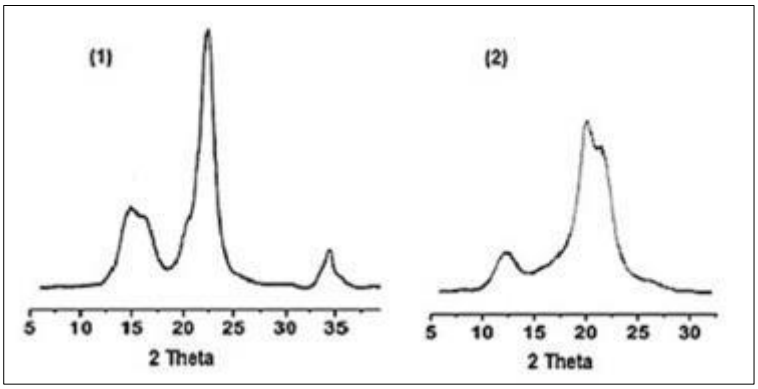

Figure 1 X-ray patterns of original (1) and mercerized (2) cotton cellulose

The diffraction patterns of the isolated and bleached wood pulps were similar to those of cotton cellulose, with the difference that the intensity of the peaks was slightly less and their width was somewhat larger. As a result, the samples

of wood pulps showed a lesser CrI value than CC (Table 2). On the other hand, acid hydrolysis of cotton cellulose to obtain microcrystalline cellulose led to an enhancement in the intensity of the peaks and an increase in CrI value due to the partial removal of the amorphous fraction from the original CC during hydrolysis.

After the mercerization of cotton cellulose, the diffraction pattern of CI allomorph turned into a diffraction pattern characteristic of CII allomorph, which contains peaks at 2Θ angles of 12.4, 20.5, 22.0, and also 34.6° (Figure 1, X-pattern 2). In addition, the intensity of these peaks was lower than the peaks of the original CI samples, which is caused by partial decrystallization during mercerization. The least structurally ordered was a sample of viscose rayon fibers (VF), the CII diffraction pattern of which had low intensive and broad peaks.

Table 6 Characteristics of cellulose samples

Sample	Allomorph	CrI	A_{sp} (N_2), m^2g	A_{sp} (H), m^2g
CC	CI	0.83 ± 0.02	1.8	5.4
MCC	CI	0.92 ± 0.02	2.2	7.1
CCM	CII	0.68 ± 0.03	0.8	3.5
KP	CI	0.78 ± 0.02	2.0	6.3
SP	CI	0.75 ± 0.03	2.1	6.5
KPM	CII	0.66 ± 0.03	0.7	3.7
VF	CII	0.54 ± 0.03	0.5	3.0

*CrI was estimated using the peak heights measurement technique of WAXS

The comparative analysis showed that the microcrystalline (MCC) sample was the most crystalline and the VF sample was the most amorphous (Table 6). However, this comparative assessment is not enough to judge the true crystallinity degree of cellulose samples. For this purpose, special studies were carried out, described below

It was found that the interaction of cellulose with liquid water is accompanied by an exothermic thermal effect, such as wetting enthalpy (Δ_wH^o). The higher the amorphicity degree of the sample, the greater will be the exothermic value of the wetting enthalpy [39]. As a result, the degrees of amorphicity (Y) and crystallinity (X) of cellulose samples were determined by the direct thermochemical method, as follows:

$$Y = \Delta_wH^o/\Delta_wH_a^o \text{ ..... (17)}$$

$$X = 1 - (\Delta_wH^o/\Delta_wH_a^o) \text{ ..... (18)}$$

where $\Delta_wH_a^o$ = -168 kJ/kg DM or – 27.2 kJ/mol AGUs is the standard wetting enthalpy of completely amorphous cellulose in the dry state [29, 39].

Table 7 Wetting enthalpy and amorphicity degree of cellulose samples

Sample	$-\Delta_wH^o$, kJ/kg	Y
CC	46.5 ± 0.2	0.28 ± 0.01
MCC	42.2 ± 0.2	0.25 ± 0.01
CCM	75.6 ± 0.2	0.35 ± 0.01
KP	58.5 ± 0.2	0.35 ± 0.01
SP	62.1 ± 0.2	0.37 ± 0.01
KPM	78.9 ± 0.2	0.47 ± 0.01
VF	104.2 ± 0.2	0.62 ± 0.01

As can be seen from the results, the thermochemical method provides the determination of the amorphicity and crystallinity degree of cellulose with a standard deviation (SD) of no more than ±0.01 (Tables 7 and 8).

Table 8 Degree (X) and index of crystallinity (CrI) for cellulose samples

Sample	X	CrI	RD, %
CC	0.72 ± 0.01	0.83 ± 0.02	15
CMC	0.75 ± 0.01	0.92 ± 0.02	23
CCM	0.55 ± 0.01	0.68 ± 0.03	24
KP	0.65 ± 0.01	0.78 ± 0.02	20
SP	0.63 ± 0.01	0.75 ± 0.03	19
KPM	0.53 ± 0.01	0.66 ± 0.03	24
VF	0.38 ± 0.01	0.54 ± 0.03	42

When CrI is estimated by existing methods (WAXS, solid-state 13C-NMR, FTIR, Raman spectroscopy, etc.), the SD is 3–5 times larger than the SD found when determining X and Y values by the proposed thermochemical method. In addition, the CrI value is poorly reproducible. The results also show that the relative deviation (RD) of the CrI value from the real X value is large and ranges from 15% for CC to 42% for VF (Table 8).

Such a large discrepancy indicates that such an estimated parameter as the crystallinity index cannot characterize the real content of crystallites in cellulose samples. In some cases, CrI measured by the same method and technique can be used only for a comparative assessment of the crystallinity of cellulose samples. On the other hand, the degree of crystallinity or amorphicity obtained using the thermochemical method describes the real supramolecular structure and provides a prediction of various important characteristics of cellulose [20, 21, 29].

It can be noted that the thermochemical method for determining the crystallinity and amorphicity degrees of cellulose samples is direct, simple, fast, precise, reliable, and reproducible. To measure the wetting enthalpy, any type of precise calorimeter can be applied, such as adiabatic, isothermal, microcalorimeter, etc. Furthermore, it does not require the use of special models, complex software, and calculations. In this method, there are no special requirements for the shape and size of the samples. They do not need to be pressed or crushed. It is possible to use cellulose samples with different morphology and type of crystalline allomorph (CI, CII, CIII, or CIV) in the form of pieces, fibers, or powders. There are only two main conditions to prepare cellulose samples for testing, namely, they must be chemically pure and completely dry. To remove the moisture from samples, a conventional vacuum drying at 378 K to constant weight can be used.

3.3. Thermodynamic Characteristics of Cellulose Samples of Different Crystalline Allomorphs

The structural studies showed that crystallites of natural celluloses have the allomorph type CI. Furthermore, it was found that the crystalline unit cell of CI can be in two distinct crystalline forms: triclinic CIα of the P_1 space group and monoclinic CIβ, of the $P2_1$ space group; where CIα form is characteristic for algae and bacterial celluloses, while more stable CIβ form is dominant in higher plants and tunicin [18, 40-42].

Three additional crystalline allomorphs: CII, CIII, and CIV, have been identified, which are attributed to structural-modified celluloses [18, 21, 41]. Samples containing CII-crystallites can be obtained by alkaline treatment of natural cellulose or by regeneration from cellulose solutions. Cellulose samples with CIII crystalline allomorph are derived from samples of CI or CII by treatment with liquid ammonia. Samples with CIV crystalline form are prepared usually by heating CIII samples in hot glycerol. Various cellulose allomorphs have different parameters of crystalline unit cells [9, 40, 41, 43, 44].

The crystalline allomorphs of cellulose differ from each other also by the shapes of crystalline unit cells. The projection of the CI-unit cell has a parallelogram shape; the CIV-unit cell has a square shape, while the unit cells of CII and CIII have a rhombic shape [9]. The content of crystalline domains in various cellulose samples (i.e., cellulose crystallinity), is different: from zero for amorphous samples to about 80% for nano-crystalline cellulose. Amorphous cellulose can be produced by ball-milling of semicrystalline cellulose samples or by saponification of amorphous cellulose acetate in a non-aqueous medium [31].

Due to the existence of different crystalline polymorphs and amorphous cellulose, various studies were performed to estimate their phase stability. The amorphous phase state is regarded as labile because the amorphous cellulose can easily crystallize in any crystalline allomorph under certain conditions. This conclusion is also confirmed by the results of thermodynamic investigations [45]. In the case of crystalline polymorphs of cellulose, the problem regarding the relative stability of the phase state is not completely resolved and remains open. A study of thermodynamic characteristics gave reason to believe that the phase state of CII is more stable than CI [21]. However, in another study, it was concluded that the stability of the phase state of various crystalline allomorphs cannot be estimated with a reasonable degree of certainty due to uncertainties in the measured characteristics [45].

Therefore, this research aimed to study the thermodynamic stability of four crystalline allomorphs of cellulose (CI, CII, CIII, and CIV), as well as amorphous cellulose (AmC). To avoid the use of uncertain indexes of crystallinity, a precise thermochemical method was proposed to determine the actual degree of crystallinity of the cellulose samples described in section 3.2. The cellulose samples having different crystalline allomorphs and various crystallinity degrees (X) were prepared (Table 9).

Table 9 Structural and thermodynamic characteristics of cellulose samples

Sample	Allomorph	X	$-\Delta_cH^o$, kJ/mol	$-\Delta_fH^o$, kJ/mol	S^o, J/mol K
MCCA	CI	0.72±0.01	2821.0±2.0	969.2±2.0	182.8 ±1.5
MCC	CI	0.75±0.01	2819.8±1.8	970.4±1.8	182.5 ±1.5
CC	CI	0.70±0.02	2821.2±1.7	969.0±1.7	182.9 ±1.9
KP	CI	0.65±0.01	2823.6±2.2	966.6±2.2	183.5 ±2.0
SP	CI	0.63±0.01	2823.8 ±2.0	966.4 ±2.0	183.7 ±2.2
BC	CI	0.28±0.01	2837.4±2.1	952.8±2.1	187.2 ±1.8
CCM	CII	0.55±0.01	2823.3±1.8	966.9±1.8	184.1 ±2.2
KPM	CII	0.53±0.01	2824.2±2.3	966.3±2.3	184.4±2.1
VF	CII	0.38±0.01	2830.0±1.7	960.2±1.7	186.0±2.0
CCA	CIII	0.37±0.01	2836.4±2.3	953.8±2.3	186.5 ±2.2
KPA	CIII	0.35±0.01	2837.0±2.0	953.2±2.0	186.7±2.0
CCAG	CIV	0.60±0.01	2825.0±2.1	965.2±2.1	184.1±2.3
KPAG	CIV	0.57±0.01	2826.1±1.9	964.1±1.9	184.4 ±2.4

The values of standard combustion enthalpy (Δ_cH^o) of these samples were determined in a calorimetric bomb as it was described in section 2.2.1. After that, the values of standard enthalpy of formation of AGUs of cellulose (Δ_cH^o) were calculated, as follows:

$$\Delta_fH^o(C_6H_{10}O_5) = 6\ \Delta_fH^o(CO_2, g) + 5\ \Delta_fH^o(H_2O, l) - \Delta_cH^o(C_6H_{10}O_5) \quad \text{.....(19)}$$

where $\Delta_fH^o(CO_2, g)$ = - 393.51 kJ/mol and $\Delta_fH^o(H_2O, l)$ = -285.83 kJ/mol are standard enthalpies of the formation of carbon dioxide and liquid water, respectively.

Literature data about the enthalpy of combustion of CI samples show that Δ_cH^o of cotton cellulose is -2827 kJ/mol [46], wood cellulose from -2823 to -2830 [44-46], and MCC from -2812 to -2821 kJ/mol [45, 48, 49]. The results obtained in this research (Table 9) are close to the literature data.

To calculate standard entropy, S^o, the data on the temperature dependence of heat capacity of cellulose samples were used [45]. As a result, the free Gibbs energy of formation was calculated:

$$\Delta_fG^o = \Delta_fH^o - T^o(S^o - \sum Si) \quad \text{.....} \quad (20)$$

where $\sum Si$ = 1199.61 J/(mol K) is the sum of standard entropies of carbon atoms (graphite), molecules of H_2 and O_2 needed for forming one AGU of cellulose; T^o = 298.15 K.

The results showed that an increase in the crystallinity degree of the samples with the same crystalline allomorph leads to a linear increase in the exothermic values of the formation enthalpy (Figure 2), and also the free Gibbs energy of formation. On the other hand, increasing the crystallinity degree causes a decrease in the positive values of the standard entropy of samples. Extrapolation of dependence S^o=f(X) to values corresponding to X = 1 and X = 0 yielded S^o_c=180 and S^o_a = 190 J/mol K for crystalline and amorphous cellulose, respectively.

With the decrease in crystallinity degree, linear dependences Δ_fH^o = f(X) and Δ_fG^o = f(X) converge at one common point, $\Delta_fH^o_a$ = -942.4 kJ/mol and $\Delta_fG^o_a$ = -642.6 kJ/mol, corresponding to X = 0. This evidences that the amorphous phase in different cellulose samples has identical thermodynamic characteristics. On the other hand, the linear extrapolation of these dependencies to the values corresponding to X = 1 gives the formation enthalpies and Gibbs energy of formation for different crystalline allomorphs, $\Delta_fH^o_c$ and $\Delta_fG^o_c$ (Table 10). Furthermore, the values of melting enthalpy (Δ_mH^o) of the cellulose crystallites with different crystalline allomorphs were calculated.

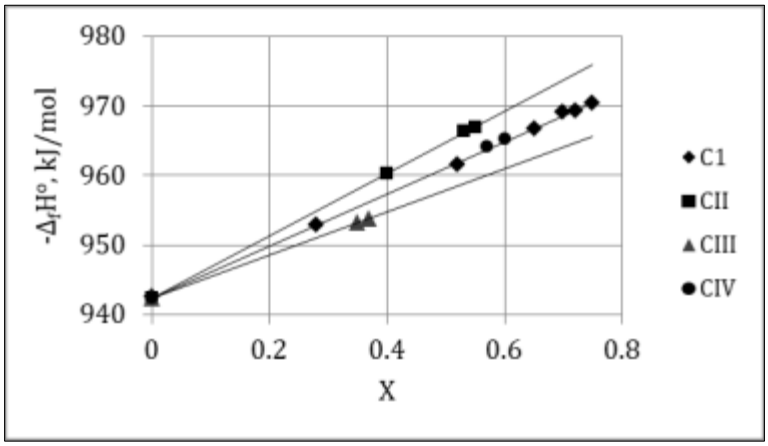

Figure 2 Dependence of enthalpy of cellulose formation on degree of crystallinity

Table 10 Thermodynamic characteristics of various crystalline allomorphs of cellulose

Allomorph	$-\Delta_fG^o_c$, kJ/mol	$-\Delta_fH^o_c$, kJ/mol	Δ_mH^o, kJ/mol
CI	676.4	979.6	37.2
CII	683.7	986.9	44.5
CIII	670.0	973.2	30.8
CIV	677.2	980.4	38.0
AmC	642.6	942.4	0

Based on the obtained results, it can be concluded regarding the thermodynamic (TD) stability of various crystalline allomorphs of cellulose and amorphous cellulose (AmC). For this purpose, the index of TD stability (SI) of these allomorphs and AmC relative to CII allomorph was calculated:

$$SI = \Delta_mH^o/\Delta_mH^o(CII) \text{ ……..(21)}$$

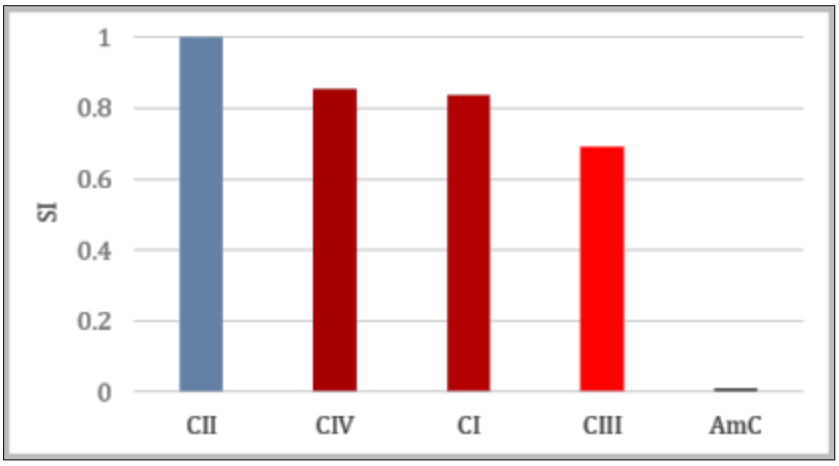

Figure 3 Index of TD stability of different crystalline allomorphs and amorphous cellulose

Thus, the thermodynamic stability of the crystalline allomorphs of cellulose and AmC decreases in the following order (Fig. 3):

$$CII > CIV \geq CI > CIII > AmC$$

On the other hand, the index of relative reactivity of the different crystalline allomorphs and AmC will decrease in the reverse order:

$$AmC > CIII > CI \geq CIV > CII$$

The obtained thermodynamic characteristics allow explain the phase transitions and reactivity of cellulose samples having different crystalline allomorphs under certain conditions. The amorphous cellulose is the most unstable and the most reactive; therefore, it can crystallize in any crystalline allomorph under certain conditions [45]. For instance, under the action of moisture, the amorphized cellulose recrystallizes in the most stable CII allomorph [31]. It is also known that after regeneration from solutions, structure of cellulose always turns to a CII crystalline allomorph.

Among various crystalline allomorphs, the CII is the most stable, whereas the CIII is the most labile. Increased phase stability of the CII crystallites leads to some problems in the cellulose application. It is known that after the transformation of crystalline structure CI of natural cellulose to CII, e.g., by mercerization, a decrease in solubility and reactivity of the sample is observed [21]. In particular, the transparency and filterability of solutions of CII samples decline due to the forming of gel particles. The presence of CII crystallites is a main factor that causes the low reactivity of cellulose at acetylation, nitration, and forming of viscose [50].

On the other hand, the transformation of crystalline structure CI of chemical pulp to labile CIII allomorph increases the reactivity of cellulose [21]. It was also discovered that high-temperature treatment of the CIII sample in the air at 480-490 K triggers the inverse transformation of CIII to CI [51], whereas after treatment in glycerol above 533 K CIII structure turns into CIV allomorph [52].

3.4. Thermodynamics of Enzymatic Hydrolysis of Cellulose

Glucose is the most abundant monosaccharide in nature [53, 54]. This monomeric carbohydrate is produced in all land plants and most algae through photosynthesis using sunlight, water, and carbon dioxide, after which it is converted into polysaccharides such as cellulose and starch [55, 56]. In addition, glucose is an integral part of disaccharide molecules such as sucrose of sugar cane and milk lactose. Glucose is the main energy source for the cells of living organisms. In addition to its physiological significance, glucose is of great importance due to its widespread use in medicine, food, and chemical industries.

Currently, glucose is produced mainly from starch by enzymatic hydrolysis [57], which has practically replaced the less profitable and harmful acid hydrolysis. Various crops can be used as a starch source for glucose production such as maize, wheat, barley, potato, etc. In the USA, maize corn starch is used almost exclusively as a feedstock for enzymatic production of glucose. However, the use of various starch sources as feedstocks for glucose production creates an acute problem because these crops are required by the food and feed industry.

Production of glucose from inedible cellulose substrates has been regarded as a promising way to obtain this valuable bioproduct without competing with the food industry. In particular, purified scraps of pulp, paper, cellulose fabrics and fibers, as well as cotton residues (e.g. linter, fuzz, etc.) and some other cellulose wastes can be used as promising and relatively cheap raw materials for enzymatic hydrolysis to produce the glucose [2]. Besides, huge amounts of pretreated cellulose-enriched plant materials (forest and agricultural wastes, bushes, grasses, etc.) can be used for enzymatic hydrolysis to convert cellulose into glucose.

Features of enzymatic hydrolysis of cellulose and cellulose-enriched materials have been discussed in many studies [53, 58-62]. Currently, to implement effective hydrolysis of cellulose, enzyme preparations were used, which include at least three types of specific enzymes:

- Endo-1,4-β-glucanases that cleave chemical glycoside bonds mainly in the amorphous domains of cellulose fibrils; as a result, the fibrils are split with the formation of small particles with a reduced degree of polymerization;
- Exo-1,4-β-glucanases that attack the reducing or non-reducing ends of the depolymerized cellulose particles by forming oligomeric products containing di- and tetra-saccharides;
- β-glucosidases that hydrolyze the oligosaccharides and convert these into glucose.

These enzymes act synergistically because endo-acting enzymes generate new chain ends for the exo-acting enzymes, which release the oligosaccharides that are converted into glucose by β-glucosidases.

Enzymatic hydrolysis of cellulose is usually carried out at pH 4.5-5.0 and temperature 298-328 K using a dose of enzyme preparation of 10-40 mg of protein per 1 g of cellulose substrate. Hydrolysis of wet cellulose is carried out faster and more completely than dried cellulose [57]. It has been found that to achieve maximum glucose concentration during enzymatic hydrolysis, the optimal loading of cellulose substrate in the aqueous enzyme system should be at least 150 g/L [63-65]. At a higher substrate loading, enzymatic hydrolysis ceases due to a significant reduction in mass transfer and inhibition of cellulolytic enzymes by a large amount of formed glucose [66].

Numerous studies have shown that when using cellulose substrates, a problem arises due to their low enzymatic digestibility. This is explained by the crystallinity of cellulose, which is considered the most important structural factor that prevents enzymatic hydrolysis [58, 67]. Therefore, it should be expected that a decrease in the crystallinity and an increase in the amorphicity of cellulose should contribute to a rise in the hydrolyzability degree of the substrate.

To answer the question of whether the crystallinity and amorphicity of cellulose are the main characteristics influencing enzymatic hydrolysis or whether this process is determined by other structural factors, additional studies are needed. Therefore, in this research, the enzymatic hydrolysis of cellulose samples with different structural characteristics was studied. In addition, thermodynamic analysis was performed to predict the enzymatic hydrolyzability of various cellulose substrates.

Various cellulose samples having crystalline structure of CI were used. Refined and bleached cotton cellulose (CC), Kraft pulp (KC), and Sulfite Pulp (SP) were purchased from Buckeye Technologies, Inc. The cellulose samples were additionally purified by extraction with boiling 2% NaOH and boiling water; then samples were washed with deionized water to a neutral pH value and squeezed to and squeezed to remove water excess. Microcrystalline cellulose (MCC) was prepared by hydrolysis of CC with boiling 2.5 N HCl for 1h; then MCC sample was washed with deionized water to a neutral pH value and squeezed to remove water excess. The cellulose of Switchgrass (SC) was isolated from the biomass by the Kürschner-Hoffer method followed by extraction with boiling 2% NaOH, washing with deionized water to a neutral pH value, and squeezing to remove water excess.

Wet cellulose samples were hydrolyzed by a commercial enzyme preparation Cellic CTec-3 (Novozymes A/S, Bagsvaerd, Denmark) containing endo-1,4-glucanases, exo-1,4-glucanases (EXG), and β-glucosidases. The dosage of Cellic CTec-3 was 30 mg per gram of dry sample. Samples containing 1 g of solids and 1 mL of 50 mM acetate buffer (pH 4.8) were placed into 50-mL polypropylene tubes and supplemented with the required amount of the enzyme and an additional buffer volume to provide the substrate loading of 150 g/L. The tubes covered with caps were incubated for 10 to 120 h at 323 K with constant shaking. Glucose concentration was determined by HPLC using an Agilent 1200 Infinity Series system (Agilent Technologies, United States) with an Amines HPX-87H column. The mobile phase was 0.005 M sulfuric acid; the flow rate was 0.6 mL/min at 318 K. Hydrolyzed samples were preliminarily filtered through a 0.45-μm nylon filter. The hydrolyzability degree (H) of the samples was calculated using the equation:

$$H = C_f/C_m \quad \text{..... (22)}$$

where C_f is the final concentration of glucose after the finish of hydrolysis of cellulose sample; C_m = 169.5 g/L is the maximum concentration of glucose achieved after the complete hydrolysis of cellulose substrate at loading of 150 g/L.

The WAXS studies were performed using a Rigaku-Ultima Plus diffractometer (see section 2.2.4). The lateral size of crystallites was calculated using the following equation [20, 21]:

$$D = \lambda/\cos\theta_{200}\,(B^2 - b^2 - \Delta^2)^{1/2} \quad \text{.....(23)}$$

where B is the width of the (200) peak (in radians); θ_{200} is Bragg's angle at the (200) peak maximum; b is the instrumental factor, and Δ is the correction on lattice distortion.

Then, the paracrystallinity degree of crystallites was calculated [20, 21]:

$$p = 4h\,(D - h)/D^2 \quad \text{.....(24)}$$

where h ≈ 0.4 nm is the thickness of external paracrystalline layers of crystallites.

Kinetic studies of enzymatic hydrolysis of cellulose samples have shown that at least three days are required to achieve the final glucose concentration and hydrolyzability degree (Figure 4).

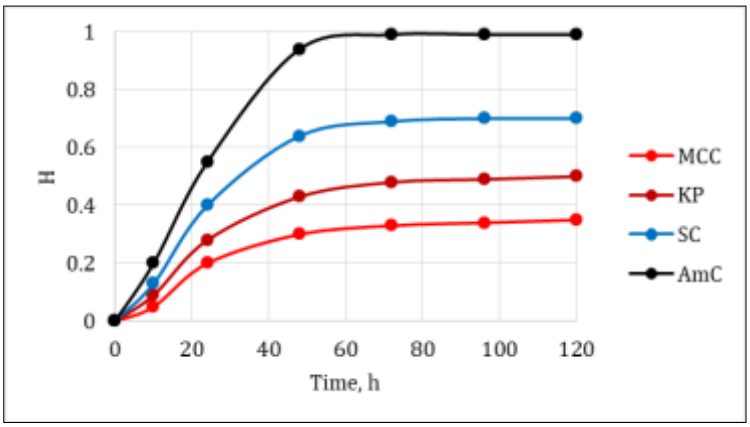

Figure 4 Kinetical curves of enzymatic hydrolysis of some wet cellulose samples

Moreover, the higher the crystallinity degree (X) of the samples, the lower the final concentration of glucose (C_f) and hydrolyzability degree (H) of these substrates (Table 11). Vice versa, the increase in amorphicity degree (Y) of cellulose leads to a rise in C_f and H values.

Table 11 Structural characteristics and hydrolyzability of cellulose samples

Cellulose	X	Y	D, nm	p	A	C_f, g/L	H
MCC	0.75	0.25	10.2	0.15	0.36	61.0	0.36
CC	0.70	0.30	8.1	0.19	0.43	72.0	0.42
KP	0.65	0.35	7.0	0.22	0.49	84.7	0.50
SP	0.63	0.37	6.1	0.25	0.53	88.5	0.52
SC	0.53	0.47	3.5	0.41	0.69	118.0	0.70
AmC	0	1	-	0	1	169.5	1

However, the hydrolyzability value of all studied semi-crystalline cellulose samples is higher than their amorphicity degree (Figure 5). This means that not only accessible amorphous domains undergo hydrolysis, but also cellulose

crystallites can be partially hydrolyzed. Such a phenomenon can be explained by the presence of accessible paracrystalline layers on the surface of cellulose nanocrystallites [20, 21].

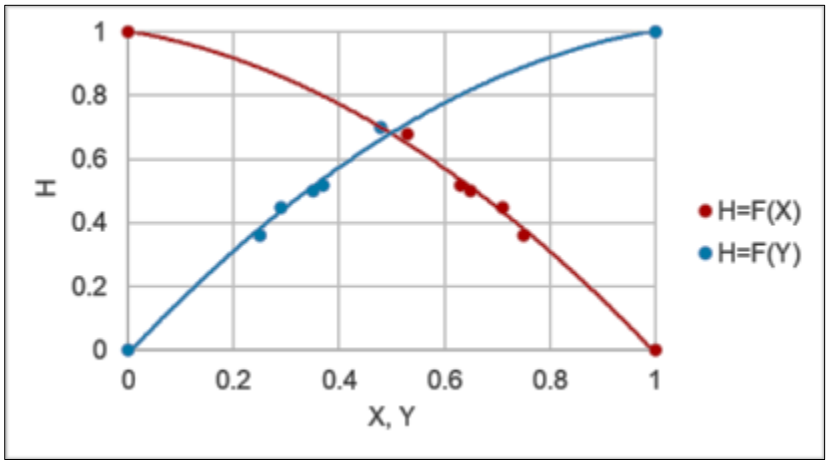

Figure 5 Dependence of final hydrolyzability of wet cellulose substrates on their crystallinity (X) and amorphicity (Y) degree

Since hydrolyzability is related to the accessibility of amorphous domains of cellulose and distorted paracrystalline layers of crystallites, the degree of accessibility of the supramolecular structure of cellulose can be expressed, as follows:

$$A = Y + pX \quad \text{.....(25)}$$

where p is the paracrystallinity degree of crystallites.

Unlike the nonlinear correlations of H from X and Y (Figure 5), the correlation of the final hydrolyzability degree (H) from the accessibility degree (A) is linear (Figure 6). In this case, a complete congruence between A and H values is observed. Moreover, these values are almost identical.

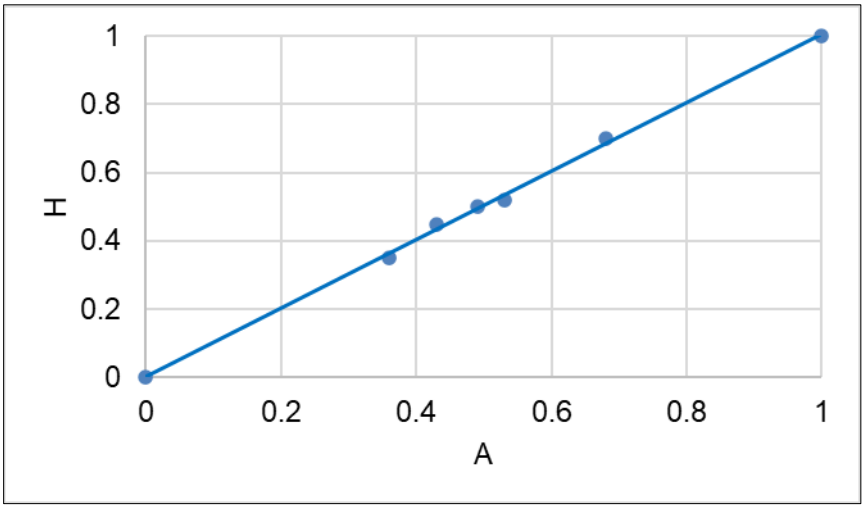

Figure 6 Dependence of final hydrolyzability of wet cellulose substrates on their accessibility degree

Thus, although the inner high-ordered domains of crystallites are resistant to enzymatic hydrolysis, outer paracrystalline layers of crystallites are distorted and therefore susceptible to hydrolysis along with the poorly ordered amorphous domains of cellulose.

After removing the outer layers, new layers should form on the surface of the crystallites and the hydrolysis process can theoretically continue slowly until the entire substrate is completely converted to glucose. However, in practice, as the hydrolysis process continues, the adsorption of glucose molecules on the developed surface of the nanocrystallites

significantly increases, which leads to the cessation of hydrolysis due to the inhibition of enzymes by the saturated adsorption layers of the sugar [68].

After determining the accessibility degree, it is possible to calculate the final glucose concentration (C_f):

$$C_f = A \times C_m \quad \text{..... (26)}$$

Where C_m = 169.5 g/L is the maximum concentration of glucose achieved after the complete hydrolysis of cellulose substrate at the loading of 150 g/L.

The disclosed features of enzymatic hydrolysis of cellulose substrates were considered in the thermodynamic analysis of this process.

An attempt to perform a thermodynamic study of the enzymatic hydrolysis of completely crystalline and completely amorphous cellulose at temperatures from 273 to 373 K using a small mass ratio of an aqueous catalyst system to cellulose (SCR) to obtain saturated glucose solutions followed by their dilution was made by Popovic et al. [69]. However, this theoretical study did not take into consideration such specific features of enzymatic hydrolysis as the negative impact of cellulose crystallinity on the hydrolysis process, limited cellulose accessibility, cessation of enzymatic hydrolysis at small SCR, the inhibition of the hydrolysis by a saturated glucose solution, low hydrolysis rate below room temperature and the inactivation of cellulolytic enzymes at temperatures above 328 K [70]. These factors were taken into account in this research when studying the thermodynamics of the real enzymatic hydrolysis process of cellulose.

As is known, for enzymatic hydrolysis, it is preferable to use wet cellulose substrates (CW). After cellulose (CEL) wetting, such substrates can contain different moles (m) of water molecules sorbed by one mole of repeating anhydroglucose units (AGUs) of cellulose:

$$CEL + m\ H_2O \rightarrow CEL \cdot m\ H_2O \quad \text{..... (27)}$$

Standard thermodynamic (TD) functions of the wet cellulose, namely, the standard formation enthalpy ($\Delta_f H$) and standard entropy (S), were calculated by the following equations:

$$\Delta_f H^o(CW) = \Delta_f H^o(CEL) + m\ \Delta_f H^o(H_2O, l) + \Delta_w H^o \quad \text{..... (28)}$$

$$S^o(CW) = S^o(CEL) + m\ S^o(H_2O, l) + \Delta_w S^o \quad \text{..... (29)}$$

where $\Delta_f H^o(CEL)$ and $S^o(CEL)$ are standard TD functions of dry cellulose (Table 12), $\Delta_w H^o$ and $\Delta_w S^o$ are standard wetting enthalpy and entropy of dry cellulose (Table 13), and **m** is the number of moles of H_2O molecules sorbed by one mole of AGUs of cellulose after saturation with water [29, 39] (Table 14).

Table 12 Standard TD functions of dry celluloses and glucose*

Cellulose	$-\Delta_c H^o$, kJ/mol	$-\Delta_f H^o$, kJ/mol	S^o, J/mol K
CR	2810.6	979.6	180.0
MCC	2819.8	970.4	182.5
CC	2821.2	969.0	182.9
KP	2823.6	966.6	183.5
SP	2823.8	966.4	183.7
SC	2826.6	963.6	184.7
AmC	2847.8	942.4	190.0
GL	2803.0	1273.0	210.0

*CR denotes CI crystallites, while AC denotes completely amorphous cellulose

Table 13 Standard wetting enthalpy and entropy of dry cellulose substrates

Cellulose	$-\Delta_w H^o$, kJ/mol	$-\Delta_w S^o$, J/mol K
CR	0	0
MCC	6.8	22.8
CC	7.9	26.5
KP	9.5	31.9
SP	10.1	33.8
SC	12.8	43.0
AmC	27.2	91.3

Table 14 Standard TD functions of wet cellulose substrates

Wet Cellulose	mH_2O/AGU	$-\Delta_f H^o$, kJ/mol	S^o, J/mol K
CR (W)	0	979.6	180.0
MCC (W)	1.1	1292.6	236.2
CC (W)	1.3	1349.5	247.0
KP (W)	1.6	1434.6	264.1
SP (W)	1.7	1463.1	269.1
SC (W)	2.1	1576.6	289.0
AmC (W)	4.5	2258.5	413.7

The wet semi-crystalline cellulose substrates were then treated with an aqueous enzyme system. As a result, the accessible amorphous domains of cellulose and outer paracrystalline surface layers of crystallites hydrolyze and form a final glucose solution containing **n** moles of H_2O per 1 mole of glucose (GL), while the inner high-ordered crystalline domains (i.e., CR) remain unhydrolyzed:

$$CEL \cdot m\ H_2O + (An + A - m)\ H_2O \rightarrow A\ (GL \times n\ H_2O) + (1\text{-}A)\ CR \quad \text{..... (30)}$$

where A is the accessibility degree of cellulose.

Standard TD functions of the final glucose solutions ($GL \times n\ H_2O$), were calculated, as follows:

$$\Delta_f H^o(GL \times n\ H_2O) = \Delta_f H^o(GL) + n\Delta_f H^o(H_2O, l) + \Delta_{dis} H^o \quad \text{..... (31)}$$

$$S^o(GL \times n\ H_2O) = S^o(GL) + n\ S^o(H_2O, l) + \Delta_{dis} S^o \quad \text{..... (32)}$$

where $\Delta_f H^o(GL)$ and $S^o(GL)$ are standard TD functions of dry crystalline glucose (Table 12), $\Delta_f H^o(H_2O, l)$ and $S^o(H_2O, l)$ are standard TD functions of liquid water, while $\Delta_{dis} H^o = 11.6$ kJ/mol and $\Delta_{dis} S^o = \Delta_{dis} H^o / T^o$ are the enthalpy and entropy of dissolution for dry crystalline glucose in water at standard temperature, T^o=298 K.

The calculation results are shown in Table 15.

Table 15 Standard TD functions of final GL solutions having final concentrations C_f

Cellulose	C_f, g/L	nH_2O/GL	$-\Delta_fH^o$, kJ/mol	S^o, J/mol K
MCC	61.0	164	48137.5	11728.9
CC	72.0	139	40991.8	9978.9
KP	84.7	118	34989.3	8508.9
SP	88.5	113	33560.2	8158.9
SC	118.0	85	25557.0	6198.9
AmC	169.5	59	18125.4	4378.9

After the determination of the standard TD functions of the wet cellulose substrates and final glucose solutions, the standard TD functions of the hydrolysis reaction can be calculated, as follows:

$$\Delta_rH^o = (1\text{-}A)\,\Delta_fH^o(CrD) + A\,\Delta_fH^o(GL \times n\,H_2O) - \Delta_fH^o(CW) - (An + A - m)\,\Delta_fH^o(H_2O, l) \quad (33)$$

$$\Delta_rS^o = (1\text{-}A)\,S^o(CrD) + A\,S^o(GL \times n\,H_2O) - S^o(CW) - (An + A - m)\,S^o(H_2O, l) \quad (34)$$

In addition, the standard Gibbs potential of the hydrolysis reaction at temperature T^o=298 K was calculated:

$$\Delta_rG^o = \Delta_rH^o - T_s\Delta_rS^o \quad (35)$$

The values of standard TD functions for the hydrolysis of cellulose substrates having various accessibility degrees are presented in Table 16.

Table 16 TD functions of the hydrolysis reaction of cellulose substrates at T^o = 298 K

Cellulose	A	Δ_rH^o, kJ/mol	$T_s\,\Delta_rS^o$, kJ/mol	Δ_rG^o, kJ/mol
MCC	0.36	-0.21	6.08	-6.29
CC	0.43	-0.22	7.01	-7.23
KP	0.49	-0.50	8.18	-8.68
SP	0.53	-0.50	8.70	-9.20
SC	0.69	-0.62	11.09	-11.71
AmC	1	-3.34	23.86	-27.20

The obtained results showed that the hydrolysis reaction of the studied cellulose samples is exothermic. Since reaction enthalpy (Δ_rH^o) is negative and the temperature-entropy factor ($T_s\Delta_rS^o$) is positive, the Gibbs potential (Δ_rG^o) of this process becomes negative, which promotes the implementation of enzymatic hydrolysis of cellulose substrates.

As is known, the optimal temperature for enzymatic hydrolysis of cellulose is T_{op}= 323 K [70, 71]. Therefore, it is advisable to perform a thermodynamic analysis of the hydrolysis process also at the mentioned optimal temperature. For this purpose, reference data on the average values of the specific heat capacity ($\hat{C}_p$) of wet cellulose, water, and aqueous solutions of glucose were used. The calculations were performed by equations (7) and (8).

The obtained results are shown in Table 17.

Table 17 TD functions of the hydrolysis reaction of cellulose substrates at T_{op}= 323 K

Cellulose	A	$\Delta_r H$, kJ/mol	$T_{op}\Delta_r S$, kJ/mol	$\Delta_r G$, kJ/mol
MCC	0.36	-0.06	6.77	-6.83
CC	0.43	-0.07	7.96	-7.90
KP	0.49	-0.07	9.34	-9.41
SP	0.53	-0.09	9.85	-9.95
SC	0.69	-1.15	11.85	-13.0
AmC	1	-3.73	25.50	-29.23

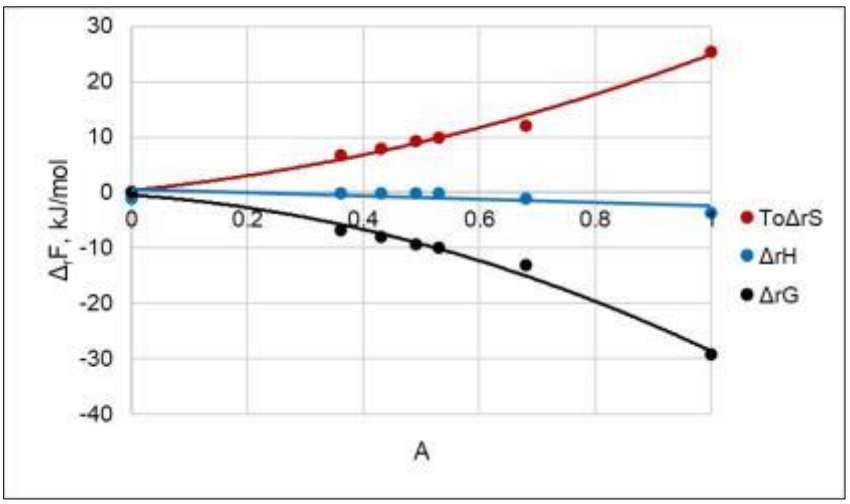

Figure 7 Dependence of TD functions of hydrolysis process on accessibility degree of cellulose substrates at optimal temperature of 323 K

Analysis of TD characteristics shows that at the optimal hydrolysis temperature of 323 K, the contribution of the temperature-entropy component to the Gibbs potential is predominant, while the Gibbs potential becomes more negative than at the temperature of 298 K. Thus, a moderate increase in temperature should promote enzymatic hydrolysis of cellulose, which is confirmed by literature data [71]. The most negative Gibbs potential was observed for the hydrolysis of the most reactive and accessible amorphous cellulose (Figure 7).

With a decrease in cellulose accessibility, the Gibbs potential of the hydrolysis reaction becomes less negative. Moreover, when extrapolated to A = 0, the Gibbs potential and other thermodynamic functions of the reaction tend to be zero due to the resistance of high-ordered crystalline domains of cellulose to enzymatic hydrolysis.

The Gibbs potential also determines the hydrolysability degree of cellulose, namely an increase in the negative value of Gibbs potential promotes the archive of a higher value of enzymatic hydrolysability (Figure 8).

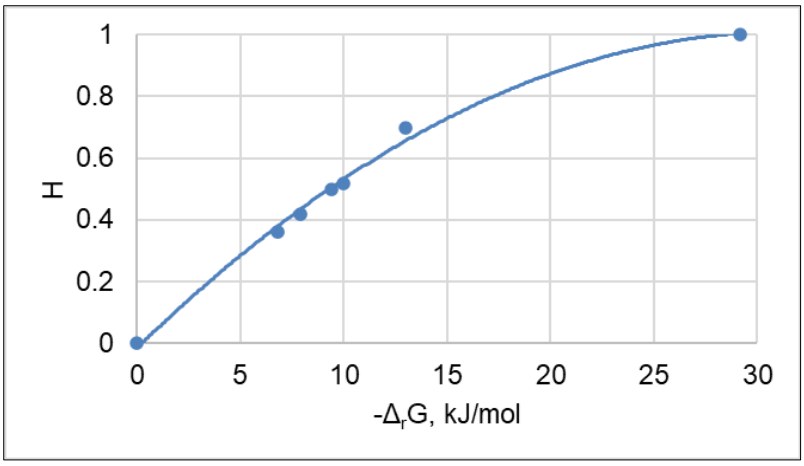

Figure 8 Dependence of cellulose hydrolysability on Gibbs potential of enzymatic hydrolysis at optimal temperature

The performed thermodynamic analysis explains the experimental results, according to which amorphization of cellulose substrates facilitates enzymatic hydrolysis.

3.5. Thermochemistry of Cellulose Alkalization

Treatment of cellulose with solutions of hydroxides of alkali metals is one of the most common methods of modification of this biopolymer. Currently, treatment with aqueous solutions of sodium hydroxide is used for the improvement of gloss, hygroscopic properties, and dyeing of cellulose fibers and fabrics, for cellulose activation and refining, as well as in the production of cellulose ethers [72-75].

It has been established that after cellulose treatment with solutions of sodium hydroxide having a concentration of less than 10% (2.8 M), the crystalline structure of CI remains unchanged [76]. However, when cellulose is alkalized with 16-20% (4.7-6.1 M) alkali solutions the hydrated hydroxide ions penetrate between [$1\bar{1}0$] planes of the crystalline lattice of CI and transform it into the swollen crystalline lattice of alkali cellulose (AlC) containing one molecule of NaOH and three molecules of H_2O per each anhydroglucose unit (AGU) in crystalline domains of cellulose.

Cellulose treatment with more concentrated sodium hydroxide solutions transforms CI crystalline lattice into lattices of other alkali cellulose types with lower volume and content of water molecules [76]. For example, cellulose alkalization with 35-40% (12.1-14.3 M) NaOH causes the formation of a crystalline lattice of AlC with the composition $AGU \cdot NaOH \cdot H_2O$, i.e., containing no more than one molecule of H_2O per AGU. An anhydrous form of AlC with the composition $AGU \cdot NaOH$ was also obtained. During alkalization, the partial decrystallization of cellulose is observed [77]. It was also established that cellulose alkalization is accompanied by an exothermic heat effect [78, 79].

After washing various alkali celluloses with water, hydroxide ions are replaced by water molecules resulting in the formation of the crystalline lattice of hydrate-cellulose, which after drying turns completely into the crystalline lattice of CII [80].

The process of formation of alkali celluloses has been studied by various methods including sorption, XRD, NMR, FTIR, Raman spectroscopy, etc. [74, 75, 79, 81-84]. Despite these studies, the mechanism of this process is still the subject of discussion. Some researchers suggest that due to the interaction of cellulose with alkali solutions, a chemical compound similar to sodium alcoholate is formed [85]. However, other researchers believe that when using aqueous solutions of alkali, the formation of such a chemical compound with cellulose is impossible, and the most probable interaction mechanism is the formation of a molecular adduct of hydrated alkali ions with cellulose [76].

$$C_6H_7O_5(OH)_3 + NaOH\ x\ mH_2O \rightarrow C_6H_7O_5(OH)_3 \cdot NaOH \cdot n\ H_2O + (m\text{-}n)\ H_2O \quad \text{..... (36)}$$

In this research, to elucidate the mechanism of the cellulose alkalization process, a thermochemical method was used to determine the heat effect or enthalpy of alkalization, as well as the standard enthalpy of the AlC formation. In addition, the thermodynamics of the cellulose etherification process was studied.

The compositions of used alkali solutions are shown in Table 18.

Table 18 The composition of 100 g alkali solutions of various concentrations (C, %)

C, %	NaOH, mol	H_2O, mol	m H_2O/NaOH
6	0.15	5.22	34.8
8	0.20	5.11	25.5
10	0.25	5.00	20.0
12	0.30	4.89	16.3
14	0.35	4.78	13.6
16	0.40	4.67	11.7
18	0.45	4.55	10.1
20	0.50	4.44	8.9
30	0.75	3.89	5.2
35	0.875	3.61	4.1
40	1.00	3.3	3.3

X-ray studies have shown that after treatment of the original cotton cellulose with an alkali concentration below 10% (2.8 M), the structure of the CI remains unchanged. When cellulose is treated with an alkali concentration higher than 10% (2.8 M), the formation of the crystalline structure of alkali cellulose (AlC) begins, accompanied by a decrease in cellulose crystallinity. If the critical alkali concentration C_{cr} =16% (4.7 M) is reached, the CI crystalline structure of the original cellulose is completely transformed into the crystalline structure of AlC, which, after washing and drying, turns completely into the CII crystalline structure with reduced crystallinity (Figures 9, 10). The appearance of CII after washing and drying the alkali-treated cellulose sample indicates the formation of the crystal structure of AlC under the influence of alkali.

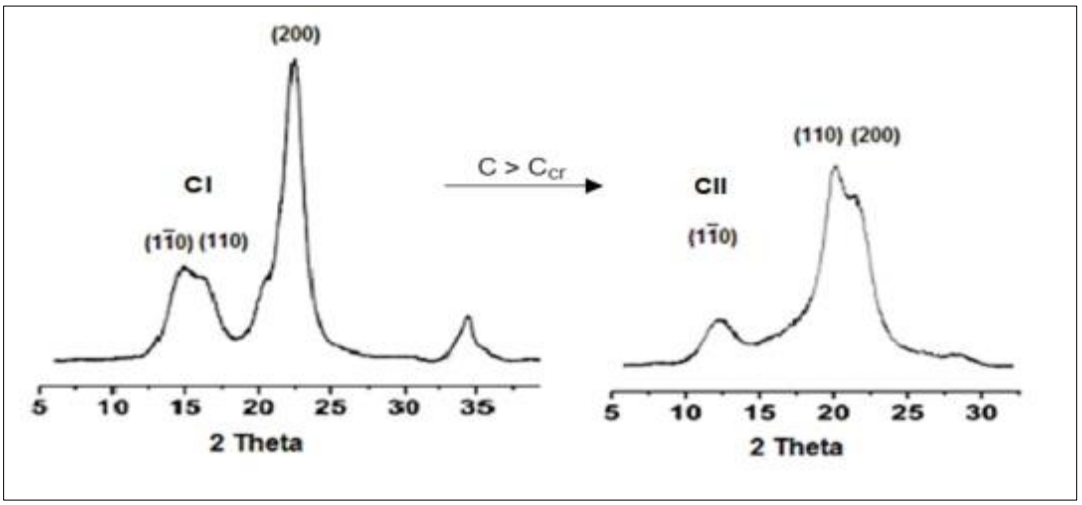

Figure 9 X-ray patterns of CI and CII

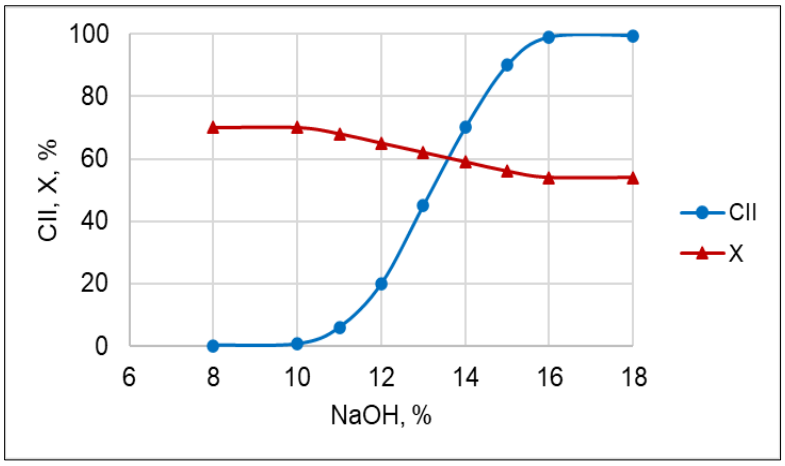

Figure 10 Dependence of CII content and crystallinity of cellulose sample on alkali concentration

A study of the absorption of hydroxide and water molecules from NaOH solutions by cellulose sample showed that AlC formed after cellulose alkalization with alkali concentration above C_{cr} =16% can contain about 1 mole of NaOH and from 1 to 4 moles of water per one AGU of cellulose [86].

Using the absorption results, the compositions of various alkali cellulose samples formed after the treatment of the original cellulose with alkali solutions having concentrations above C_{cr} were assessed (Table 19).

Table 19 Estimated composition of various alkali celluloses

C, %	AlC Label	AGU, mol	NaOH, mol	n H_2O, mol
16	AlC 1	1	1	4
18	AlC 2	1	1	4
20	AlC 3	1	1	4
30	AlC 4	1	1	2
35	AlC 5	1	1	1
40	AlC 6	1	1	1

The alkalization process with the formation of alkali celluloses with modified crystalline structures can be described, as follows:

$$AGU + NaOH \; x \; m \; H_2O \rightarrow AGU \cdot NaOH \cdot n \; H_2O + (m-n) \; H_2O + \Delta_{al}H^o \quad \text{..... (37)}$$

where $\Delta_{al}H^o$ is the standard enthalpy of alkalization

The results showed that the formation of AlC 4-6 is accompanied by a higher value of exothermic enthalpy of alkalization than the formation of AlC 1-3 (Figure 11).

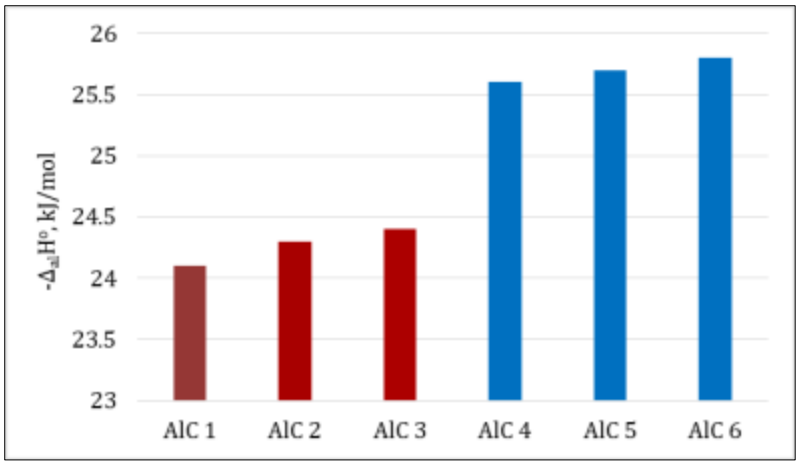

Figure 11 Enthalpy of cellulose alkalization with the formation of various alkali celluloses

Another significant thermodynamic characteristic is the standard enthalpy of the formation of alkali cellulose from one AGU and alkali solution containing **m** moles H_2O per 1 mol of NaOH (Table 18).

Following Hess's law, the standard enthalpy of the formation of alkali cellulose was calculated, as follows:

$$\Delta_f H^o(AlC) = \Delta_f H^o(CC) + \Delta_f H^o(Alkali) - (m\text{-}n)\,\Delta_f H^o(H_2O) + \Delta_{al} H^o \quad \text{..... (38)}$$

where $\Delta_f H^o$ (CC) = -969 kJ/mol is the standard enthalpy of formation of 1 mole AGU of original cotton cellulose [40], $\Delta_f H^o(H_2O)$ = -285.83 kJ/mol is the standard enthalpy of formation of liquid water, $\Delta_{al} H^o$ is the enthalpy of alkalization (Figure), while the standard enthalpy of formation of an alkali solution is:

$$\Delta_f H^o(Alkali) = \Delta_f H^o(NaOH) + m\,\Delta_f H^o(H_2O) + \Delta_{ds} H^o \quad \text{..... (39)}$$

Note: $\Delta_f H^o(NaOH)$ = -426.6 kJ/mol is the standard enthalpy of formation of crystalline NaOH and $\Delta_{ds} H^o$ is the enthalpy of dissolution of 1 mole NaOH in **m** moles H_2O [87].

The results of the calculations are shown in Tables 20 and 21.

Table 20 Standard enthalpy of formation of alkali solutions

C, %	m	$-\Delta_{ds} H^o$, kJ/mol	$-\Delta_f H^o$ (Alkali), kJ/mol
16	11.7	42.6	3813
18	10.1	42.5	3356
20	8.9	42.0	3012
30	5.2	38.2	1951
35	4.1	34.5	1633
40	3.3	31.0	1401

Table 21 Standard enthalpy of formation of various alkali celluloses

AlC Label	n	$-\Delta_{al}H$, kJ/mol	$-\Delta_fH$ (AlC), kJ/mol
AlC 1	4	24.1	2605
AlC 2	4	24.3	2605
AlC 3	4	24.4	2605
AlC 4	2	25.6	2030
AlC 5	1	25.7	1742
AlC 6	1	25.8	1738

It was found that with an increase in the number of H_2O molecules (n) in the AlC composition, the exothermic value of formation enthalpy of alkali cellulose increases linearly (Figure 12).

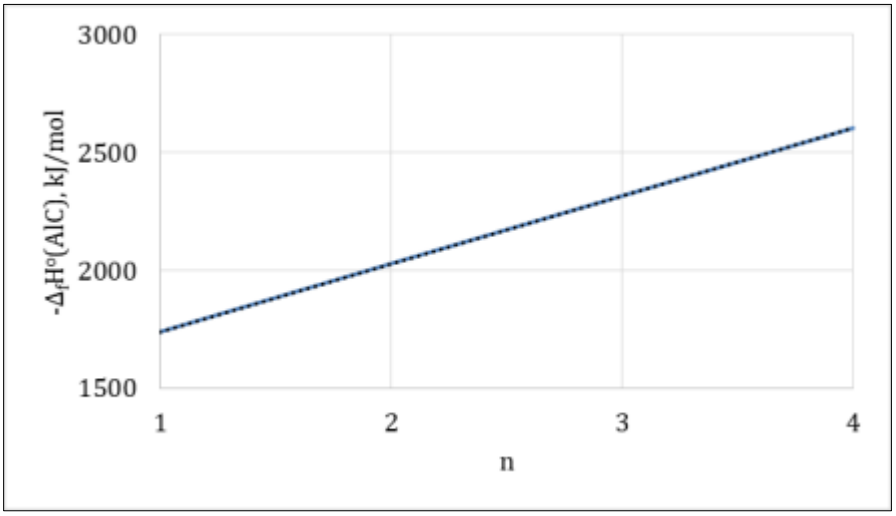

Figure 12 Dependence of formation enthalpy of alkali cellulose on the number of H_2O molecules

This dependence is expressed by the following equation:

$$\Delta_fH^o(AlC) = -288.3\ n - 1452 \quad \text{..... (40)}$$

From the presented results it follows that the enthalpy of the formation of various alkali celluloses, $\Delta_fH^o(AlC)$, is exothermic, and thus, the process of cellulose alkalization is energetically favorable. Thus, alkalization is a physicochemical process of forming a molecular adduct of hydrated hydroxide ions with cellulose. In addition, since the exothermic enthalpy of alkalization, $\Delta_{al}H^o$, at the formation of the AlC 4-6 has the highest value, these alkali celluloses should be more reactive than the AlC 1-3 samples.

3.6. Thermochemistry of Cellulose Etherification

The various cellulose ethers are known such as methylcellulose (MC), ethylcellulose (EC), hydroxyethylcellulose (HEC), carboxymethylcellulose (CMC), etc. The cellulose ethers are thermoplastic polymers. The softening temperature (T_s) of these ethers decreases with increasing length of substituent and degree of substitution (DS). Therefore, at the same DS T_s of ET is lower than that of MC.

Another characteristic feature of cellulose ethers is their ability to dissolve in cold water. The sodium salt of CMC dissolves in water if the degree of substitution is 0.5 and above, HEC at DS 0.8 and above, EC at DS 1.1 and above, and MC at DS 1.3 and above. Due to these features, cellulose ethers are widely used as thickeners of water-based paints and coatings.

The synthesis of cellulose ethers is carried out in two main steps. The first step is cellulose alkalization to turn it into alkali cellulose (AlC) having increased accessibility to etherifying reagents. It was found that to obtain more reactive and accessible AlC, the initial cellulose should be alkalized with alkali solutions having a concentration above 30%, and preferably 40% [86]. The second step is the etherification of obtained AlC.

Consider as an example the process of production of methylcellulose (MC). The first step of this process is cellulose alkalization with a 40% NaOH solution at room temperature, after which the excess alkali is removed to obtain a mass ratio of alkali to cellulose of 3:1. The resulting AlC 6 is kept in the air at 310 K for 1-2 h

Then, in the second step, AlC 6 is methylated with methyl chloride:

$$C_6H_7O_2(OH)_3 \cdot NaOH \cdot H_2O + (x-1)\,NaOH + x\,CH_3Cl \rightarrow C_6H_7O_2(OH)_{3-x}(OCH_3)_x + x\,NaCl + (1+x)\,H_2O \quad \text{..... (41)}$$

where **x** is the degree of substitution (DS) of MC. It was taken into account that real MC samples designated as MC-1 and MC-2 have DS of 1.3 and 1.8, respectively.

Taking into consideration the equation of the etherification process, the enthalpy of the methylation reaction of AlC 6 can be calculated, as follows:

$$\Delta_rH^o = \Delta_fH^o(MC) + x\Delta_fH^o(NaCl) + (1+x)\,\Delta_fH^o(H_2O) - \Delta_fH^o(AlC\ 6) - (x-1)\,\Delta_fH^o(NaOH) - x\,\Delta_fH^o(CH_3Cl) \quad \text{..... (42)}$$

where $\Delta_fH^o(AlC\ 6) = -1738$ kJ/mol is the standard enthalpy of formation of AlC 6 (see Table 21), while $\Delta_fH^o(NaCl)$, $\Delta_fH^o(NaOH$, $\Delta_fH^o(CH_3Cl)$, and $\Delta_fH^o(H_2O)$ is the standard enthalpy of formation of the corresponding substance (Table 22).

Table 22 Standard enthalpy of formation of various substances

Substance	$-\Delta_fH^o$, kJ/mol
NaCl (cr)	410.9
NaOH (cr)	426.6
CH_3Cl (g)	83.7
H_2O (l)	285.83
CO_2 (g)	393.51

The standard enthalpy of formation $\Delta_fH^o(MC)$ for MC 1 and MC 2 samples was calculated from the standard combustion enthalpy $\Delta_cH^o(MC)$ of these samples:

$$\Delta_fH^o(MC) = (6+x)\,\Delta_fH^o(CO_2) + (5+x)\,\Delta_fH^o(H_2O) - \Delta_cH^o(MC) \quad \text{..... (43)}$$

where $\Delta_fH^o(CO_2)$ and $\Delta_fH^o(H_2O)$ are the standard enthalpy of formation of corresponding substances (Table 22), while the experimental value of standard combustion enthalpy of $\Delta_cH^o(MC1) = -3706$ kJ/mol, and $\Delta_cH^o(MC2) = -4036$ kJ/mol, respectively.

Then, the standard enthalpy of formation of MC1 $\Delta_fH^o(MC1) = -967.3$ kJ/mol, and MC 2 $\Delta_fH^o(MC2) = -977.0$ kJ/mol

As a result, the following values of enthalpy of the methylation reaction of AlC 6 to obtain methylcellulose samples were calculated using eq. (37).

For MC 1 (x=DS = 1.3): $\Delta_rH^o(MC\ 1) = -184$ kJ/mol.

For MC 2 (x=DS = 1.8): $\Delta_rH^o(MC\ 2) = -287$ kJ/mol.

Since the enthalpy values of the methylation reaction of AlC 6 were quite exothermic, this means that the methylation reaction is energetically advantageous. Moreover, obtaining methylcellulose with a higher degree of substitution is preferable.

3.7. Thermodynamics of Cellulose Esterification

As known, each repeating unit of cellulose contains three hydroxyl functional groups, one primary at C6 and two secondary groups at C2 and C3, which impart increased hydrophilicity to cellulose materials [20, 21]. This limits the use of cellulose in such applications as the creation of waterproof and vapor-proof materials, the production of hydrophobic fillers and reinforcements compatible with hydrophobic polymers, hydrophobic coatings, paints, adhesives, and other hydrophobic materials.

A more reliable method of cellulose hydrophobization is its chemical modification, especially esterification by replacing hydroxyl groups with hydrophobic substituents [88, 89]. For example, it was shown that acetylation of cellulose increases its hydrophobicity and leads to a decrease in the sorption of water vapor [90]. As for other cellulose esters, when moving from acetates to higher cellulose esters, the hydrophobicity of cellulose derivatives rises [91]. In addition, when passing from monoester to triester, a noticeable enhancement of hydrophobicity is observed, since in this event non-polar groups replace all three hydroxyls in the repeating unit.

Due to their performance properties, cellulose esters can be used in the production of hydrophobic plastics, compositions of hydrophobic coatings, adhesives, and other hydrophobic materials [88, 89, 92].

Cellulose esterification can be carried out under heterogeneous and homogeneous conditions. Homogeneous esterification is considered preferable because it proceeds fairly uniformly in the solvent medium that dissolves cellulose. To synthesize esters, the original cellulose is dissolved in a suitable solvent and esterified with various acyl reagents at elevated temperatures [88, 93-95]. The X-ray studies showed that the structural state of cellulose esters is mesomorphous, which is characterized by the presence of diffuse reflections typical of amorphized polymers, having a local order in the arrangement of repeating units [88, 93].

In this study, various mesomorphous mono-, di-, and triesters of cellulose were investigated. Theoretically, each repeating unit of these esters with a molar mass **M** should contain acyl substituents with a different number of carbon atoms, $\mathbf{N_c}$ (Table 23).

Table 23 The studied cellulose esters

Cellulose Esters	Name	N_c	Formula of unit	M
Monoacetate	MAC	2	$C_8H_{12}O_6$	204
Diacetate	DAC	4	$C_{10}H_{14}O_7$	246
Triacetate	TAC	6	$C_{12}H_{16}O_8$	288
Monopropionate	MPC	3	$C_9H_{14}O_6$	218
Dipropionate	DPC	6	$C_{12}H_{18}O_7$	274
Tripropionate	TPC	9	$C_{15}H_{22}O_8$	330
Monobutyrate	MBC	4	$C_{10}H_{16}O_6$	232
Dibutyrate	DBC	8	$C_{14}H_{22}O_7$	302
Tributyrate	TBC	12	$C_{18}H_{28}O_8$	372
Monovalerate	MVC	5	$C_{11}H_{18}O_6$	246
Divalerate	DVC	10	$C_{16}H_{26}O_7$	330
Trivalerate	TVC	15	$C_{21}H_{34}O_8$	414
Monohexanoate	MHC	6	$C_{12}H_{20}O_6$	260
Dihexanoate	DHC	12	$C_{18}H_{30}O_7$	358

Trihexanoate	THC	18	$C_{24}H_{40}O_8$	456
Monoenanthane	MEC	7	$C_{13}H_{22}O_6$	274
Dienanthate	DEC	14	$C_{20}H_{34}O_7$	386
Trienanthate	TEC	21	$C_{27}H_{46}O_8$	498

The one repeating unit of cellulose esters can be described by the following general formulas.

Monoesters (M): $C_{(8+n)}H_{(12+2n)}O_6$

Diesters (D): $C_{(10+2n)}H_{(14+4n)}O_7$

Triesters (T): $C_{(12+3n)}H_{(16+6n)}O_8$

where n is the number of CH_2-groups in one substitute.

Then, the combustion process of one mole of repeating units of esters will be the following:

For M: $C_{(8+n)}H_{(12+2n)}O_6$ (s) + (8+1.5n) O_2 (g) = (8+n) CO_2 (g) + (6+n) H_2O (l) + Δ_cH^o(M)

For D: $C_{(10+2n)}H_{(14+4n)}O_7$ (s) + (10+3n) O_2 (g) = (10+2n) CO_2 (g) + (7+2n) H_2O (l) + Δ_cH^o(D)

For T: $C_{(12+3n)}H_{(16+6n)}O_8$ (s) + (12+4.5n) O_2 (g) = (12+3n) CO_2 (g) + (8+3n) H_2O (l) + Δ_fH^o (T)

Accordingly, standard enthalpies of the formation of these esters can be calculated, as follows.

For M: Δ_fH^o(M) = (8+n) Δ_fH^o(CO_2, g) + (6+n) Δ_fH^o(H_2O, l) - Δ_fH^o(M) ..... (44)

For D: Δ_fH^o(D) = (10+2n) Δ_fH^o(CO_2, g) + (7+2n) Δ_fH^o(H_2O, l) - Δ_fH^o(D) ..... (45)

For T: Δ_fH^o(T) = (12+3n) Δ_fH^o(CO_2, g) + (8+3n) Δ_fH^o(H_2O, l) - Δ_fH^o(T) ..... (46)

where Δ_fH^o(CO_2, g) = -393.51(kJ/mol) is the standard enthalpy of the formation of gaseous carbon dioxide, and Δ_fH^o (H_2O, l) = -285.83 (kJ/mol) is the standard enthalpy of the formation of liquid water.

The experimentally determined thermodynamic (TD) characteristics of cellulose esters [96] are collected in Table 24.

Table 24 Thermodynamic characteristics of cellulose esters

Ester	Formula of unit	N_c	$-\Delta_cH^o$, kJ/mol	$-\Delta_fH^o$, kJ/mol
MAC	$C_8H_{12}O_6$	2	3747.6	1115.5
DAC	$C_{10}H_{14}O_7$	4	4647.5	1288.4
TAC	$C_{12}H_{16}O_8$	6	5547.4	1461.3
MPC	$C_9H_{14}O_6$	3	4408.0	1134.5
DPC	$C_{12}H_{18}O_7$	6	5968.3	1326.3
TPC	$C_{15}H_{22}O_8$	9	7528.6	1518.2
MBC	$C_{10}H_{16}O_6$	4	5068.3	1153.4
DBC	$C_{14}H_{22}O_7$	8	7289.0	1364.2
TBC	$C_{18}H_{28}O_8$	12	9509.7	1575.1
MVC	$C_{11}H_{18}O_6$	5	5728.7	1172.4

DVC	$C_{16}H_{26}O_7$	10	8609.8	1402.1
TVC	$C_{21}H_{34}O_8$	15	11490.9	1631.9
MHC	$C_{12}H_{20}O_6$	6	6389.1	1191.3
DHC	$C_{18}H_{30}O_7$	12	9930.6	1440
THC	$C_{24}H_{40}O_8$	18	13472.1	1688.7
MEC	$C_{13}H_{22}O_6$	7	7049.5	1210.3
DEC	$C_{20}H_{34}O_7$	14	11251.4	1477.9
TEC	$C_{27}H_{46}O_8$	21	15453.2	1745.7

Studies have shown that these TD characteristics are linear functions of the number of carbon atoms (N_c) in the acyl substituents (Table 25).

Table 25 Correlation equations $\Delta H^o = f(N_c)$

Ester	Equations	R^2
M	$-\Delta_c H^o = 660\ N_c + 2427$	0.96
	$-\Delta_f H^o = 19\ N_c + 1077$	0.96
D	$-\Delta_c H^o = 660\ N_c + 2006$	0.98
	$-\Delta_f H^o = 19\ N_c + 1212$	0.98
T	$-\Delta_c H^o = 660\ N_c + 1585$	0.97
	$-\Delta_f H^o = 19\ N_c + 1347$	0.97

These results show that increasing the length of the substituent and degree of substitution (DS) contributes to enhancing the exothermic enthalpy of ester formation. Thus, cellulose esterification to increased DS value, especially by long-chain acyl reagents, is thermodynamically favorable.

3.7.1. Thermochemistry of Cellulose Acetates and Nitrates

Among diverse cellulose esters, two esters, acetates, and nitrates of cellulose are the most widespread and have practical importance. Cellulose acetate also called acetylcellulose (AcC) with various DS is used in the production of thermoplastics, electronic device housings, cigarette filters, semi-permeable and separating membranes, optical films, spectacle frames, heat- and rot-resistant fabrics, self-cleaning materials, protective coatings, and other materials [97].

For their part, nitrocelluloses (NIC) are used in the production of plastics, membranes, films, protective coatings, adhesives, paints, varnishes and enamels, powders, rocket fuels, explosives, etc. [98]. It was shown that the application area of use depends on the degree of substitution (DS) of the nitrocellulose samples [99, 100]. If DS is less than 1.5, this type of NIC can only be used to produce paints, varnishes, and enamels. NIC having DS between 1.5 and 2.4 is used in the production of plastics and membranes. If DS > 2.4, then this type of NIC can be used to produce smokeless powder, rocket propellants, and explosives.

It is known that depending on the conditions, the cellulose esterification can proceed in two main topochemical directions: bulk and local. In the bulk process, the reagent quickly reacts with amorphous domains, and more slowly with cellulose crystallites, resulting in cellulose decrystallization and forming an amorphous ester with a mesomorphous structure [88, 101]. The starting crystallinity degree of cellulose affects the rate of esterification reaction but has little impact on the final degree of substitution.

In the bulk acetylation, the initial cellulose material is activated, placed in a suitable organic liquid (e.g., acetic acid, methylene chloride, etc.), and then treated with acetic anhydride in the presence of a small amount of catalyst, usually sulfuric or perchloric acid [102]. The reaction is performed at temperatures of 303-313 K for 60 min, at a ratio of the

acetylating system to cellulose 10-20. The bulk esterification typically produces cellulose triacetate (TAC). To obtain an ester with a lower degree of substitution, additional acid treatment of the primary TAC is carried out.

The cellulose is bulk nitrated with concentrated nitric acid alone or with various nitrating systems, such as mixtures of nitric acid, sulfuric acid, and water; nitric acid, phosphoric acid, and phosphoric anhydride; nitric acid, acetic acid, and acetic anhydride; nitric acid and its salts; nitric acid and dichloromethane; nitric acid and ether; etc. [103, 104]. However, for the industrial production of NIC, only mixtures of nitric with sulfuric acid and water are used. The cellulose nitration can be carried out at temperatures of 273-313 K for 30-60 min, at a ratio of the nitrating system to cellulose 30-50. The DS value of the resulting NC is adjusted by changing the composition of the reaction mixture, especially the water content.

The second topochemical direction is the local esterification of only the most accessible amorphous domains of cellulose, while crystallites (CR) remain almost unreacted. This local nitration process is observed if the nitrating mixtures contain an increased amount of water. On the other hand, local acetylation can be achieved by treating cellulose with acetic anhydride in the presence of liquids that are not solvents of either cellulose or its acetate.

Although the chemical aspects of cellulose esterification are well known, its thermochemistry is poorly understood. It has only been established that bulk esterification processes up to high DS values can be exothermic. The thermal effects of local esterification have not been studied at all. This article is devoted to solving this problem.

Samples of cellulose esters with various DS values were synthesized by methods of bulk and local esterification [105].

The standard thermodynamic (TD) characteristics of the studied samples of cellulose esters and cellulose are presented in Table 26.

Table 26 Standard TD characteristics of studied samples

Sample	DS	$-\Delta_cH^o$, kJ/mol	$-\Delta_fH^o$, kJ/mol
CR	0	2810.6	979.6
CC	0	2821.2	969.0
AmC	0	2847.8	942.4
AC-1	1.11	3841.5	1136.0
AcC-2	2.12	4808.6	1310.2
AcC-3	2.80	5364.0	1430.1
AcC-4	0.60	3385.1	1049.2
MAC	1	3747.6	1115.5
SAC	1.5	4197.5	1202.0
DAC	2	4647.5	1288.4
TAC	3	5547.4	1461.3
NIC-1	0.97	2801.4	847.3
NIC-2	2.03	2744.5	749.1
NIC-3	2.85	2700.2	669.1
NIC-4	0.60	2819.2	883.6
MNC	1	2799.4	848.3
SNC	1.5	2776.6	799.9
DNC	2	2753.7	751.5
TNC	3	2708.0	654.7

From Tables 10 and 26, it follows that the melting enthalpy of CI crystallites (CR) is:

$$\Delta_m H^o = \Delta_f H^o(AmC) - \Delta_f H^o(CR) = 37.2 \text{ (kJ/mol)} \ldots\ldots\ldots\ldots\ldots\ldots (47)$$

For comparison with the obtained TD characteristics, some literature data were presented in Table 27, and Figures 13, 14. As can be seen, the obtained experimental results are confirmed by literature data.

Table 27 Literature data on the standard TD characteristics of samples

Sample	$-\Delta_c H^o$, kJ/mol	$-\Delta_f H^o$, kJ/mol	Reference
Cotton linter	2824.1	966.1	[46]
AmC	2842.8	947.4	[47]
	2845.3	945.0	[105]
	2847.8	942.4	[40, 96]
AcC, DS=1.60	4263.5	1243.3	[106]
AcC, DS= 2.36	4890.2	1431.9	[106]
AcC. DS=2.83	5316.1	1510.0	[106]
DNC	2751.6	753.3	[46]
NIC, DS=2.12	2748.2	742.7	[46]
TNC	2709.4	653.0	[46]

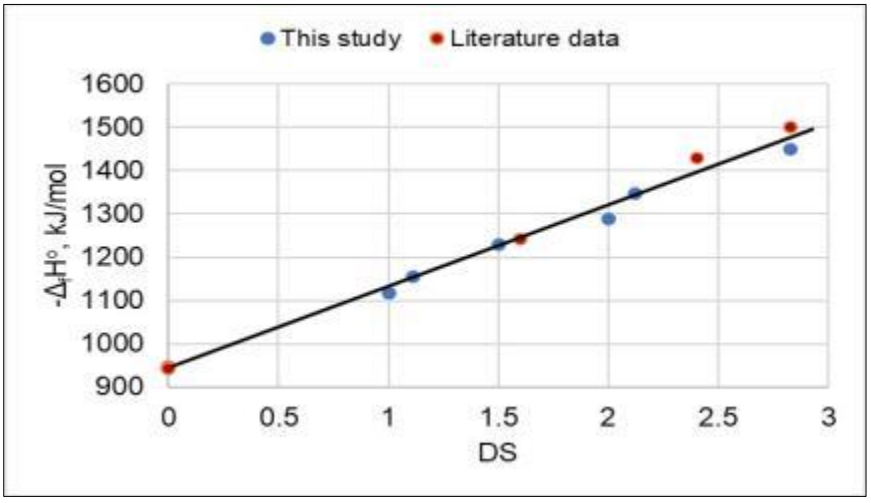

Figure 13 Dependence of standard formation enthalpy on the degree of substitution of AcC samples

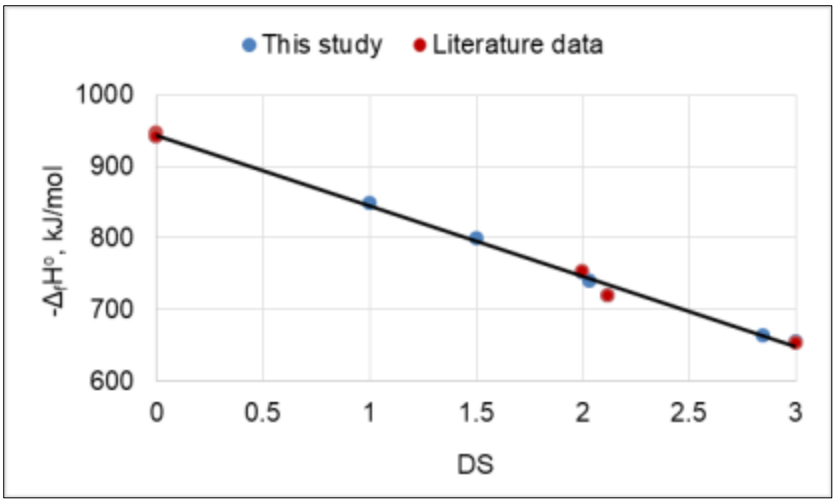

Figure 14 Dependence of standard formation enthalpy on the degree of substitution of NIC samples

In addition to the standard TD functions of cellulose and its ethers, reference data on the standard enthalpies of formation of reagents and low-molecular esterification products were also used for thermodynamic calculations of cellulose esterification (Table 28).

Table 28 The standard formation enthalpies of substances

Liquid Substance	Symbol	$-\Delta_fH^o$, kJ/mol
Nitric Acid	HNO_3	173
Acetic Anhydride	AcAn	625
Acetic Acid	AcAc	484.5
Water	H_2O	285.83

Bulk esterification of cellulose

The bulk process is accompanied by the decrystallization (melting) of cellulose crystallites and the esterification of the formed amorphous cellulose with the formation of amorphous esters having a mesomorphous structural state. This bulk process can be described by the following TD equation:

$$\Delta_rH^o(CC) = \Delta_rH^o(AmC) + X\,\Delta_mH^o \quad \text{..... (48)}$$

where $\Delta_rH^o(CC)$ and $\Delta_rH^o(AmC)$ are enthalpies of bulk esterification of initial cotton cellulose (CC) and amorphous cellulose (AmC), respectively; Δ_mH^o=37.2 (kJ/mol) is the melting enthalpy of CI crystallites, while X=0.7 is the crystallinity degree of CC sample.

To calculate the enthalpy of bulk acetylation of AmC , the following equation was used:

$$\Delta_rH^o(AmC)_{AC} = \Delta_fH^o(AcC) + DS\,[\Delta_fH^o(AcAc) - \Delta_fH^o(AcAn)] - \Delta_fH^o(AmC) \quad \text{..... (49)}$$

On the other hand, the enthalpy of bulk nitration of AmC was calculated, as follows:

$$\Delta_rH^o(AmC)_{NC} = \Delta_fH^o(NIC) + DS\,[\Delta_fH^o(H_2O) - \Delta_fH^o(HNO_3)] - \Delta_fH^o(AmC) \quad \text{..... (50)}$$

The formation enthalpies of CC and AmC samples, cellulose esters with various DS, as well as reagents (AcAn and HNO_3), and low-molecular-weight products of esterification (AcAc and H_2O), are presented in Tables 26 and 28.

The resulting enthalpies of bulk esterification reactions of cotton cellulose are shown in Tables 29 and 30.

Table 29 Enthalpies of bulk acetylation of CC to different DS

*AcC (B)	DS	Δ_rH^o, kJ/mol
MAC (B}	1	-7.1
SAC (B)	1.5	-22.9
DAC (B)	2	-28.6
TAC (B)	3	-71.1

Symbol (B) denotes the bulk reaction

Table 30 Enthalpies of bulk nitration of CC to different DS

*NIC (B)	DS	Δ_rH^o, kJ/mol
MNC (B}	1	7.3
SNC (B)	1.5	-0.8
DNC (B)	2	-9.3
TNC (B)	3	-25.1

Symbol (B) denotes the bulk reaction

As can be seen from Table 30, the reaction of bulk nitration of cellulose to DS of 1.5 is endothermic; therefore, its implementation requires an influx of thermal energy from the outside. However, it is known that bulk nitration of the cellulose also proceeds when the reaction system is cooled to relatively low temperatures when the supply of thermal energy from the outside is difficult [107]. In this case, the only possibility for the feasibility of bulk nitration reaction of the cellulose sample is that the absolute value of the temperature-entropy factor must be greater than the absolute value of reaction enthalpy, so that the Gibbs potential of this reaction becomes negative, namely:

$$[T\Delta_rS] > [\Delta_rH] \text{ and } \Delta_rG = (\Delta_rH - T\Delta S) < 0$$

where Δ_rG is the Gibbs potential of cellulose nitration, and T is the reaction temperature.

Thus, thermodynamic analysis shows that the process of bulk nitration of cellulose with a weak nitrating system to DS up to 1.5 can only be implemented if the temperature-entropy component is positive and makes a predominant contribution to the Gibbs potential. On the other hand, when cellulose is nitrated with concentrated nitrating systems to DS above 1.5, the reaction enthalpy becomes exothermic. Thus, when the bulk nitration of cellulose is carried out to increased DS values, the feasibility of this reaction is determined mainly by the contribution of enthalpy to the negative Gibbs potential.

Unlike nitration, the bulk acetylation of cellulose is always an exothermic process, regardless of the achieved DS value (Table 29). Moreover, the more DS, the higher the exothermic heat effect of this reaction. It can be also noted that an increase in reaction entropy and temperature-entropy factor will facilitate the implementation of the acetylation process. However, if the reaction entropy is negative, then the following conditions must be fulfilled for the implementation of bulk acetylation of cellulose:

$$[\Delta_rH] > [T\Delta_rS] \text{ and } \Delta_rG = (\Delta_rH - T\Delta_rS) < 0$$

Anyway, the feasibility of bulk acetylation is determined mainly by the exothermic enthalpy of this reaction.

The results also showed that bulk acetylation is accompanied by the release of significantly more heat energy than the bulk nitration process (Figure 15).

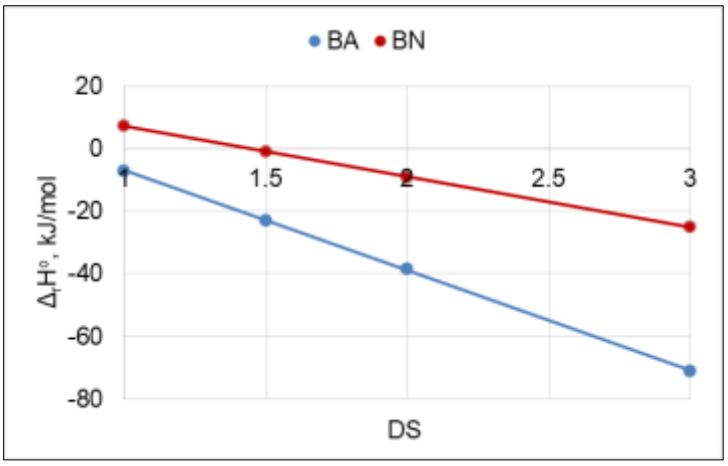

Figure 15 Dependence of reaction enthalpy on the degree of substitution for bulk acetylation (BA) and bulk nitration (BN) of cotton cellulose

Local esterification of amorphous domains of cellulose

Consider the local esterification process of only the most accessible amorphous domains of cellulose when the crystallites (CR) of the sample remain unreacted. These local reactions of acetylation and nitration, e.g., of cotton cellulose (CC) can be described, as follows:

$$CC + Y\ DS_a\ AcAn \rightarrow Y\ AC + Y\ DS_a\ AcAc + X\ CR \quad \text{..... (51)}$$

$$CC + Y\ DS_a\ HNO_3 \rightarrow Y\ NC + Y\ DS_a\ H_2O + X\ CR \quad \text{..... (52)}$$

where Y= 0.3 is the amorphicity degree, and X=0.7 is the crystallinity degree of CC; DS_a is the degree of substitution of amorphous domains of CC, which can vary from 1 to 3.

To calculate the enthalpy of the local acetylation reaction of cotton cellulose, $\Delta_rH^o(CC)_{AC}$, the following TD equation was used:

$$\Delta_rH^o(CC)_{AC} = X\ \Delta_fH^o(CR) + Y\ \Delta_fH^o(AcC) + Y\ DS_a\ [\Delta_fH^o(AcAc) - \Delta_fH^o(AcAn)] - \Delta_fH^o(CC) \quad \text{..... (53)}$$

On the other hand, the TD equation to calculate the enthalpy of the local nitration reaction of cotton cellulose, $\Delta_rH^o(CC)_{NC}$, is the following:

$$\Delta_rH^o(CC)_{NC} = X\ \Delta_fH^o(CR) + Y\ \Delta_fH^o(NIC) + Y\ DS_a\ [\Delta_fH^o(H_2O) - \Delta_fH^o(HNO_3)] - \Delta_fH^o(CC) \quad \text{..... (54)}$$

The obtained results are shown in Tables 31 and 32.

Table 31 Enthalpies of local acetylation reaction of CC

*AcC (L)	DS_a	DS	Δ_rH^o, kJ/mol
MAC {L}	1	0.30	-9.4
SAC (L)	1.5	0.45	-14.1
DAC (L)	2	0.60	-18.8
TAC (L)	3	0.90	-28.8

Symbol (L) denotes the local reaction; DS=Y DS_a is the average substitution degree

Table 32 Enthalpies of local nitration reaction of CC

*NIC (L)	DS_a	DS	Δ_rH^o, kJ/mol
MNC (L}	1	0.30	-5.1
SNC (L)	1.5	0.45	-7.5
DNC (L)	2	0.60	-10.0
TNC (L)	3	0.90	-14.8

Symbol (L) denotes the local reaction; DS=Y DS_a is the average substitution degree

From Figure 16 it follows that the local acetylation is a much more exothermic process than the local nitration.

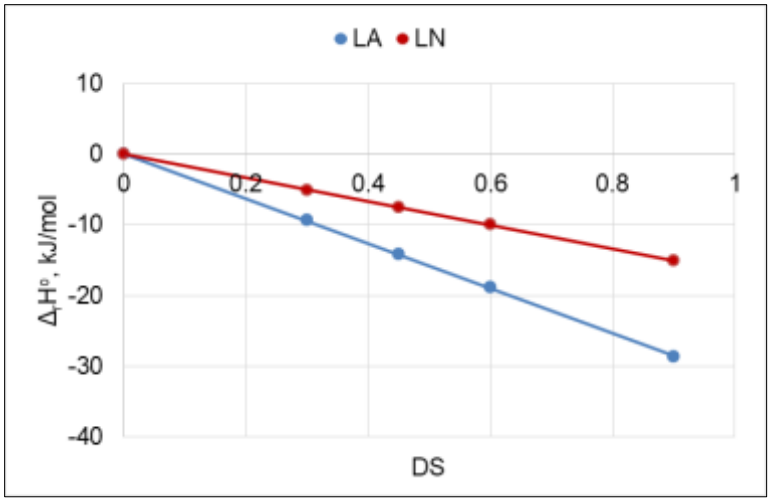

Figure 16 Dependence of reaction enthalpy on the average degree of substitution for local acetylation (LA) and local nitration (LN) of cotton cellulose

Since the local esterification is an exothermic process, then the feasibility of this process is probably determined by the contribution of reaction enthalpy to negative Gibbs potential:

A specific feature of locally modified cellulose esters is the localization of substituents in amorphous domains, due to which the resulting material is a block copolymer of amorphous ester and crystalline cellulose. Since the ester groups are hydrophobic and cellulose crystallites are water resistant, such a copolymer should be significantly less hydrophilic than cellulose. Therefore, it can be expected that the local esterification method will find a practical application for the inexpensive hydrophobization of cellulose fibers, films, fabrics, and papers, as well as cellulose-based fillers and excipients, namely, powdered, microcrystalline, and nano celluloses.

3.8. Thermodynamics of Cellulose Oxidation

Oxidation is one of the most common processes in cellulose chemistry and technology. Cellulose is sensitive to the action of atmospheric oxygen at elevated temperatures, as a result of which its hydroxyl groups are oxidized and converted into carbonyl groups, such as aldehyde, and keto-groups [102]. The non-selective cellulose oxidation by oxygen at increased temperatures is usually accompanied by the depolymerization of this biopolymer. Other oxidants causing non-selective oxidation of cellulose are chlorine, hypochlorites, permanganates, peroxides, etc. [108, 109]. In addition to non-selective methods, there are also methods of selective oxidation of cellulose with the formation of dialdehyde cellulose, carboxyl celluloses, and some other oxycelluloses [108, 109].

To obtain dialdehyde cellulose (DAC), cellulose is selectively oxidized with sodium or potassium periodate solutions at room or elevated temperature in a dark flask [110]. As a result of the oxidation of two secondary hydroxyl groups of AGUs, two aldehyde groups are formed in their place (Figure 17). This process is accompanied by the opening of the glucopyranose cycle.

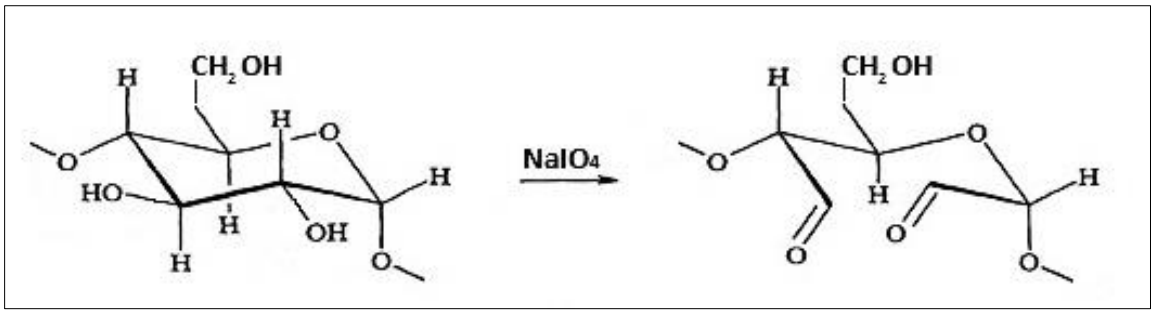

Figure 17 Scheme of cellulose oxidation with periodate in DAC

Mono-carboxyl cellulose (MCAC) is prepared via selective oxidation of the primary hydroxyl groups of AGUs of cellulose by nitrogen dioxide or dinitrogen tetroxide at elevated temperatures in a vacuum flask (Figure 18) [108, 109]. Solutions of dinitrogen tetroxide in some organic solvents (CH_2Cl_2, $CHCl_3$, CCl_4, etc.) are also used to prepare MCAC [111].

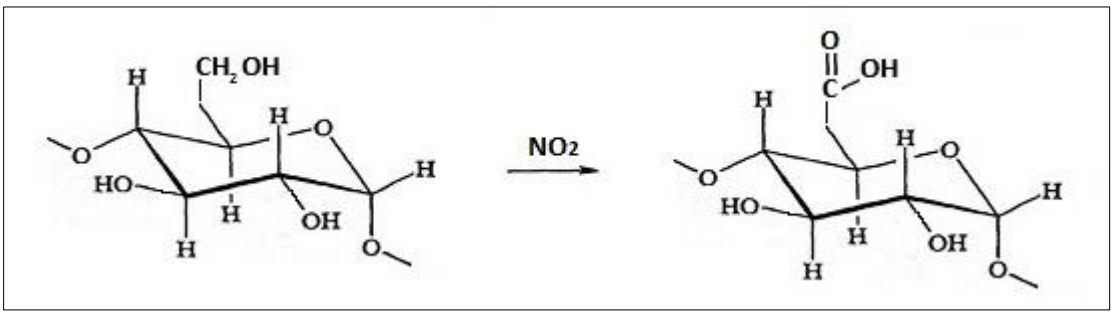

Figure 18 Scheme of cellulose oxidation with nitrogen dioxide in MCAC

To obtain MCAC, cellulose can also be oxidized with TEMPO or sodium persulfate [108].

To prepare dicarboxyl cellulose (DCAC), cellulose is sequentially oxidized with periodate and sodium chlorite [108, 109]. Tri-carboxyl cellulose (TCAC) can be prepared by sequentially oxidizing cellulose with periodate, sodium chlorite, and nitrogen dioxide [108, 112].

Oxidized celluloses, DAC, MCAC, DCAC, and TCAC, are used as carriers for various therapeutic active substances (TAS). Due to the presence of aldehyde groups, DAC can bind TAS-containing amino groups, e.g. proteolytic enzymes, amino acids, and other TAS [108].

The acidic functional groups of carboxylated celluloses contribute to the ion binding of TAS containing basic functional groups, e.g., lysine, antibiotic gentamicin, etc. [108, 113]. In addition, they can chemosorb various inorganic and organic cations. Additional applications of oxy-celluloses are their use in formulations of anti-acne remedies, fungicides, and some other medicaments. Moreover, various oxy-celluloses exhibit good hemostatic ability [108, 114].

Considering the great scientific and practical importance of oxidized celluloses, it is advisable to study their thermodynamic characteristics and the thermodynamics of various oxidation reactions of cellulose.

Some characteristics of the studied samples are shown in Table 33.

Table 33 Characteristics of oxy-cellulose samples*

Sample	Name	Formula	M	O, %
Mono-carboxyl cellulose	MCAC	$C_6H_8O_6$	176	54.54
Di-carboxyl cellulose	DCAC	$C_6H_8O_7$	192	58.33
Tri-carboxyl cellulose	TCAC	$C_6H_6O_8$	206	62.13
Dialdehyde cellulose	DAC	$C_6H_8O_5$	160	50.00
Mono-keto cellulose	MKEC	$C_6H_8O_5$	160	50.00
Di-keto cellulose	DKEC	$C_6H_6O_5$	158	50.63

*The Formula refers to the repeating units of oxy-cellulose; M is the molecular weight of one repeating unit; O, % is the oxygen percentage in oxy-cellulose.

The combustion process of oxy-cellulose having formula $C_xH_yO_z$ can be described, as follows:

$$C_xH_yO_z + (x + 0.25y - 0.5z)\ O_2 \rightarrow x\ CO_2 + 0.5y\ H_2O + \Delta_cH^o \quad \text{..... (55)}$$

where Δ_cH^o is the standard combustion enthalpy of oxy-cellulose (Table 34).

After determining the Δ_cH^o values, the formation enthalpy (Δ_fH^o) of oxy-cellulose samples can be calculated using the known equation:

$$\Delta_fH^o(C_xH_yO_z) = x\ \Delta_fH^o(CO_2, g) + 0.5y\ \Delta_fH^o(H_2O, l) - \Delta_cH^o \quad \text{..... (56)}$$

Table 34 Thermodynamic characteristics of oxy-cellulose samples

Name	OI	$-\Delta_cH^o$, kJ/mol	$-\Delta_fH^o$, kJ/mol	$-\Delta_rH^o$, kJ/mol
AmC	0	2848	942	0
MCAC	2	2427	1077	919
DCAC	3	2253	1251	1342
TCAC	5	1832	1387	2263
DAC	1	2600	904	497
MKEC	1	2600	904	497
DKEC	2	2353	865	993

The oxidation reaction of cellulose can be represented in two stages. In the first stage, the oxidizer splits off oxygen, and in the second stage, the oxygen of the oxidizer oxidizes cellulose into oxy-cellulose. Considering that the amorphous domains (ADs) of cellulose are predominantly subject to oxidation, the second stage of oxidation reaction of one mole of AGUs of ADs or AmC can be described as follows:

$$C_6H_{10}O_5 + (z - 0.5\ y)\ O \rightarrow C_6H_yO_z + (5 - 0.5\ y)\ H_2O \quad \text{..... (57)}$$

The standard enthalpy of the oxidation reaction of one mole of AGUs of ADs or AmC was calculated as follows:

$$\Delta_rH^o = \Delta_fH^o(\text{Oxy-C}) + (5 - 0.5\ y)\ \Delta_fH^o(H_2O) - \Delta_fH^o(\text{AmC}) - (z - 0.5\ y)\ \Delta_fH^o(O) \quad \text{..... (58)}$$

where Δ_fH^o(Oxy-C), Δ_fH^o(AmC), $\Delta_fH^o(H_2O)$, and $\Delta_fH^o(O)$ are standard formation enthalpies of oxy-cellulose, amorphous cellulose, liquid water, and atomic oxygen, respectively.

The number of moles of oxygen atoms required to obtain 1 mole of oxy-cellulose is called the oxygen index (OI), which can be found from the oxidation reaction:

$$OI = z - 0.5y \quad \text{..... (59)}$$

where z and y denote the number of oxygen and hydrogen atoms, respectively, in the formula of repeating unit of oxy-cellulose.

The analysis of the obtained results showed that increasing the oxygen index (OI) leads to an enhancement in the exothermic value of the oxidation reaction, thereby promoting the oxidation process and the formation of oxy-cellulose (Figure 19).

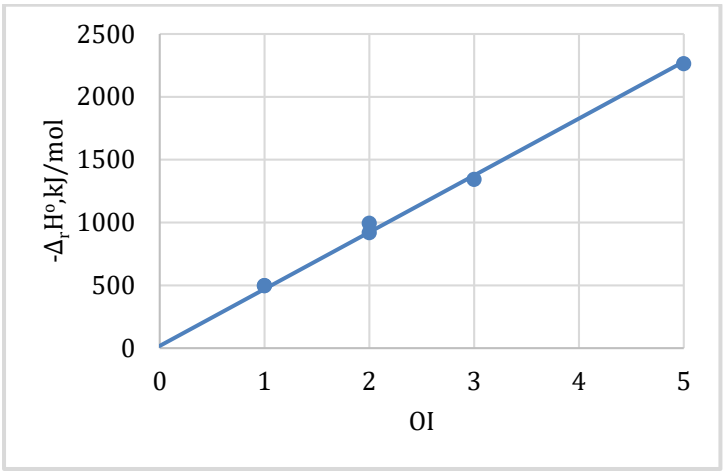

Figure 19 Dependence of enthalpy of oxidation on the oxygen index

In addition, the following rule has been discovered for carboxyl celluloses: with an increase in the number of carboxyl groups the enthalpy of the oxidation reaction becomes more exothermic (Figure 20).

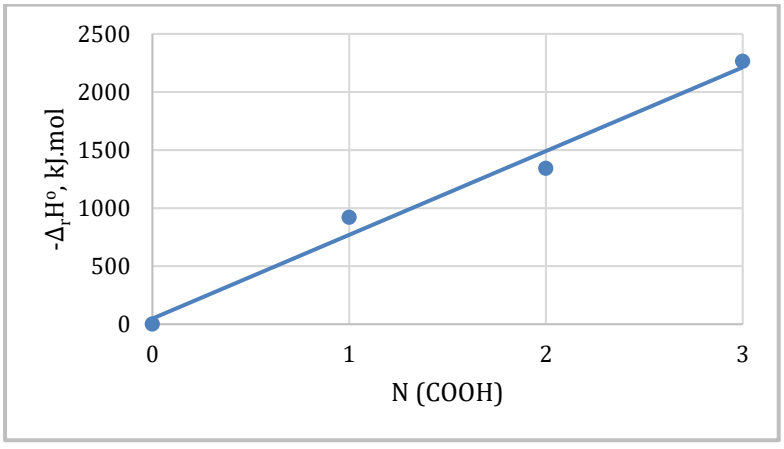

Figure 20 Dependence of enthalpy of oxidation on the number of carboxylic groups in carboxyl cellulose samples

Thus, the thermodynamical analysis showed that oxidizing cellulose with the formation of various oxy-celluloses is an energetically favorable process.

4. Conclusion

This review article discusses the chemical thermodynamics and thermochemistry of biomass, cellulose, and its derivatives such as ethers, esters, and oxycelluloses. The great potential of using thermodynamic methods in the study of biomass, cellulose, and its derivatives was demonstrated. In particular, new data on the structural characteristics of cellulose and its crystalline allomorphs were obtained. Thermodynamic features of hydrolysis, alkalization, etherification, esterification, and oxidation processes of cellulose were studied and thermodynamically regularities of these processes were discovered.

Compliance with ethical standards

Disclosure of conflict of interest

The author of this paper declares that there is no conflict of interest.

References

[1] Klotz IM, Rosenberg RM. Chemical Thermodynamics. Basic Concepts and Methods. Whiley & Sons Inc: Hoboken; 2008.

[2] Ioelovich. M. Recent findings and the energetic potential of plant biomass as a renewable source of biofuels – A Review. Bioresources, 2015; 10: 1879-1914.

[3] Lee S, Speight JG, Loyalka SK. Handbook of Alternative Fuel Technologies. CRC Press: Boca Raton; 2007.

[4] Klemm D, Heublein B, Fink H.-P, Bohn A. Cellulose: fascinating biopolymer and sustainable raw material. Angew. Chem. 2005; 44: 2-37.

[5] Čuček L, Martin M, Grossmann IE, Kravanja Z. Energy, water and process technologies integration for the simultaneous production of ethanol and food from the entire corn plant. Comp. Chem. Eng. 2011; 35: 1547-1557.

[6] Blankenship RE. Molecular Mechanisms of Photosynthesis, 2nd ed. John Wiley & Sons: Oxford; 2014;

[7] Zeller-Powel CE. Defining biomass as a source of renewable energy: The life-cycle carbon emissions of biomass energy and a survey and analysis of biomass definitions in states' renewable portfolio standards. Federal law, and proposed legislation. Master's Thesis. University of Oregon: Eugene; 2011.

[8] Ioelovich M. Analysis of energy potential of switchgrass biomass. Biomass, 2024; 4: 740-750.

[9] Ioelovich M. Cellulose Nanostructured Natural Polymer. LAP: Saarbrücken; 2014.

[10] Young RA, Rowell RM. Cellulose: Structure, Modification and Hydrolysis. Wiley: New York; 1986.

[11] Sjöström E. Wood Chemistry, Fundamentals and Applications. Academic Press: London; 1993.

[12] Fengel D, Wegener G. Wood Chemistry, Ultrastructure, Reactions. Walter de Gruyter: Berlin, New York; 1984.

[13] Ioelovich M, Leykin A. Formation of nanostructure of microcrystalline cellulose. Cellulose Chem. Technol. 2006; 40: 313-317.

[14] Wilkie JS. Carl Nägeli and the fine structure of living matter. Nature, 1961; 190: 1145-1150.

[15] Zugenmaier P. Contribution to the historical development of macromolecular chemistry – exemplified on cellulose. Cellulose Chem. Technol. 2009; 43: 351-378.

[16] Meyer KH, Misch L. Positions des atomes dans le nouveau modèle spatial de la cellulose**.** Helv. Chim. Acta, 1937; 20: 232-244.

[17] Gardner KH, Blackwell J. The structure of native cellulose. Biopolymers, 1974; 13: 1975–2001.

[18] O'Sullivan A. Cellulose: the structure slowly unravels. Cellulose, 1997; 4: 173-207.

[19] Krässig H. Cellulose: Structure, Accessibility and Reactivity. Gordon and Breach Publ.: Amsterdam; 1993.

[20] Ioelovich M. Models of supramolecular structure and properties of cellulose. J. Polym. Sci. Ser. A, 2016; 58: 925-943.

[21] Ioelovich M. Progress in Characterization of Cellulose and Cellulose Esters. Eliva Press: Chisinau; 2023.

[22] Sluiter JB, Ruiz RO, Scarlata CJ, et al. Compositional analysis of lignocellulosic feedstocks - review and description of methods. *J. Agricult. Food Chem. 2010;* 58: 9043-9053.

[23] Ioelovich M. Thermodynamics of cellulose esterification. World J. Adv. Res. Rev. 2023; 19: 225–232.

[24] Kelley KK, Parks G S, Huffman HM. A new method for extrapolating specific heat curves of organic compounds below the temperature of liquid air. J. Phys. Chem. 1929; 33: 1802–1805

[25] Harjunen P, Lehto VP, Koivisto M, et al. Determination of amorphous content of lactose samples by solution calorimetry. Drug Dev. Ind. Pharm. 2004; 30: 809–815.

[26] Timmermann EO. Multilayer sorption parameters: BET or GAB values. Colloid Surface A, 2003; 220: 235-260.

[27] Ioelovich M. Energy potential of natural, synthetic polymers and waste materials – A review. Acad. J. Polym. Sci. 2018; 1: 15.

[28] Ioelovich M. Comparison of methods for calculation of combustion heat of biopolymers. American J. Appl. Sci. Eng. Technol. 2016; 1: 63-67.

[29] Ioelovich M. Application of thermochemical method to determine the crystallinity degree of cellulose materials. Appl. Sci. 2023; 13: 2-11.

[30] Maier G, Zipper P, Stubičar M, Schurz J. Amorphization of different cellulose samples by ball milling. Cellul. Chem. Technol. 2005, 39, 167–177.

[31] Ioelovich, M. Preparation, characterization and application of amorphized cellulose - A review. Polymers, 2021; 13: 1-21.

[32] Park S, Baker JO, Himmel ME, et al. Cellulose crystallinity index: Measurement techniques and their impact on interpreting cellulase performance. Biotechnol. Biofuels, 2010; 3: 1–10.

[33] Terinte N, Ibbett R, Schuster KC. Overview on native cellulose and microcrystalline cellulose I structure studied by X-ray diffraction (WAXD): Comparison between measurement techniques. Lenzing. Ber. 2011; 89: 118–131.

[34] Rongpipi S, Ye D, Gomez ED, Gomez EW. Progress and opportunities in the characterization of cellulose - An important regulator of cell wall growth and mechanics. Front. Plant Sci. 2019; 9: 1–28.

[35] Madhushani WH, Priyadarshana RWIB, Ranawana SRW, et al. Determining the crystallinity index of cellulose in chemically and mechanically extracted banana fiber for the synthesis of nanocellulose. J. Nat. Fibers, 2022; 19: 7973–7981.

[36] Leong SL, Tiong SIX, Siva SP, et al. Morphological control of cellulose nanocrystals via sulfuric acid hydrolysis based on sustainability considerations: An overview of the governing factors and potential challenges. J. Environ. Chem. Eng. 2022; 10: 1–20.

[37] Ioelovich M. Heat effects of interaction between cellulose and various polar liquids. SITA, 2011; 13: 35-44.

[38] Ioelovich M. Study of cellulose interaction with various liquids. SITA, 2017; 19: 10-15.

[39] [Ioelovich M. Physicochemical methods for determination of cellulose crystallinity. ChemXpess, 2016; 9: 245-251.

[40] Ioelovich M. Study of thermodynamic properties of various allomorphs of cellulose. ChemXpess, 2016; 9: 259-265.

[41] Zugenmaier P. Crystalline cellulose and cellulose derivatives. Characterization and structures. Springer-Verlag: Berlin, Heidelberg; 2008.

[42] Sugiyama J, Vuong R, Chanzy H. Electron diffraction study on the two crystalline phases occurring in native cellulose from an algal cell wall. Macromolecules, 1991; 24: 4168-4175.

[43] Zugenmaier P. Conformation and packing of various crystalline cellulose fibers. Progress in Polym.Sci., 2001; 26: 341-1417.

[44] Langan P, Nishiyama Y, Chanzy H. X-ray structure of mercerized cellulose II at 1 Å resolution. Biomacromolecules, 2001; 2: 410-416.

[45] Goldberg RN, Schliesser J, Mittal A, et al. A thermodynamic investigation of the cellulose allomorphs: cellulose(am), cellulose I,(cr), cellulose II(cr), and cellulose III(cr). J. Chem. Thermodyn., 2015; 81: 184-226.

[46] Jessup RS, Prosen EJ. Heats of combustion and formation of cellulose and nitrocellulose. J. Res. Nat. Bur. Stand., 1050; 44; 387–393.

[47] Uryash VF, Larina VN, Kokurina NY, Novoselova NV. The thermochemical characteristics of cellulose and its mixtures with water. J. Phys. Chem., 2010; 84: 1023-1029.

[48] Colbert C, Xiheng H, DR. Enthalpy of combustion of microcrystalline cellulose. J. Res. Natl. Bur. Stand., 2009; 86: 655-660.

[49] Nelson ML. Energy relationships among crystal lattice types of cellulose. (Thesis). Tulane University; 1957.

[50] Ioelovich M. Crystalline structure of alkali-celluloses and its influence on viscose forming process. Wood Chem., 1990; 2: 8-15.

[51] Wada M. *In situ* observation of the crystalline transformation from cellulose III_I to I_β. Macromolecules, 2001; 34: 3271-3275.

[52] Kulshreshth K. A review of the literature on the formation of cellulose IV, its structure, and its significance in the technology of rayon manufacture. J. Text. Inst., 1979; 70: *13-18.*

[53] Ioelovich M. Specific features of enzymatic hydrolysis of cellulose. WJARR, 2024; 22: 381–392.

[54] Domb AJ, Kost J, Wiseman D. Handbook of Biodegradable Polymers*. CRC Press: Boca Raton; 1998.*

[55] Kamide K. Cellulose Products and Cellulose Derivatives: Molecular Characterization and its Applications*. Elsevier: Amsterdam; 2005.*

[56] Pfister B, Zeeman SC. Formation of starch in plant cells. Cell. Mol. Life Sci., 2016; 73: 2781–2807.

[57] Fellows PJ. Food Processing Technology. Woodhead Publishing: Cambridge; 2016.

[58] Ioelovich M, Morag E. Effect of cellulose structure on enzymatic hydrolysis. Bioresources, 2011; 6: 2818-2834

[59] Horn SJ, Vaaje-Kolstad G, Westereng B, Eijsink VG. Novel enzymes for the degradation of cellulose. Biotech. Biofuel., 2012; 5: 45-57.

[60] Bansal P, Vowell BJ, Hall M, et al. Elucidation of cellulose accessibility, hydrolysability and reactivity as the major limitations in the enzymatic hydrolysis of cellulose. Biores. Technol., 2012; 107: 243-250.

[61] Amândio MST, Rocha JMS, Xavier AMRB. Enzymatic hydrolysis strategies for cellulosic sugars production to obtain bioethanol from eucalyptus globulus bark. Fermentation, 2023; 9, 241: 1-19.

[62] Reis CER, Junior NL, Bento HBS, et al. Process strategies to reduce cellulase enzyme loading for renewable sugar production in biorefineries. Chem. Eng. J., 2023, 451 (2),138690, 1-10.

[63] Ioelovich M, Morag E. Study of enzymatic hydrolysis of pretreated biomass at increased solids loading. Bioresources, 2012; 7: 4672-4682.

[64] Pino MS, Rodríguez-Jasso RM, Michelin M, et al. Bioreactor design for enzymatic hydrolysis of biomass under the biorefinery concept. Chem. Eng. J., 2018; 347: 119–136.

[65] Da Silva AS, Espinheira RP, Teixeira RSS, et al. Constraints and advances in high-solids enzymatic hydrolysis of lignocellulosic biomass: A critical review. Biotechnol. Biofuels, 2020; 13, 58: 1-28.

[66] Xiao Z, Zhang X, Gregg DJ, Saddler JN. Effects of sugar inhibition on cellulases and beta-glucosidase during enzymatic hydrolysis of softwood substrates. Appl. Biochem. Biotechnol., 2004;113-116:1115-1126.

[67] Hall M, Bansal P, Lee J, et al. Cellulose crystallinity – A key predictor of the enzymatic hydrolysis rate. FEBS Journal, 2010; 277: 1571-1582.

[68] Xiao Z, Zhang X, Gregg DJ, Saddler JN. Effects of sugar inhibition on cellulases and beta-glucosidase during enzymatic hydrolysis of softwood substrates. Appl. Biochem. Biotechnol., 2004;113-116:1115-1126.

[69] Popovic M, Woodfield BF, Hansen LD. Thermodynamics of hydrolysis of cellulose to glucose from 0 to 100 °C: cellulosic biofuel applications and climate change implications. J. Chem. Thermodynamics, 2019; 128: 244-250.

[70] Ioelovich M. Thermodynamics of enzymatic hydrolysis of cellulose. World J. Adv. Res. Rev., 2024; 21: 577–586.

[71] Kabir F, Lu-Kwang Ju. On optimization of enzymatic processes: temperature effects on activity and long-term deactivation kinetics. Process Biochem., 2023; 130: 734-746.

[72] Valášek P., Müller M., Šleger V., et al. Influence of alkali treatment on the microstructure and mechanical properties of Coir and Abaca fibers. Materials, 2021: 14, 2636: 1-20.

[73] Shahril S.M., Ridzuan M.J.M., Abdul-Majid M.S., et al Alkali treatment influence on cellulosic fiber from Furcraea foetida as potential reinforcement of polymeric composites. J. Mater. Res. Technol., 2022; 19: 2567-2583.

[74] Tatsumi D., Kanda A., Kondo T. Characterization of mercerized cellulose nanofibrils prepared by aqueous counter collision process. J. Wood Sci., 2022; 68**,** 13: 1-9.

[75] Yokota S., Nishimoto A., Kondo T. Alkali-activation of cellulose nanofibrils to facilitate surface chemical modification under aqueous conditions. J. Wood Sci., 2022; 68, 14: 1-7.

[76] Goychman A.S., Solomko V.P. High- Molecular Inclusion Compounds. Science: Kiev; 1982.

[77] Ferro M., Mannu A., Panzeri W., et al. An integrated approach to optimizing cellulose mercerization. Polymers, 2020; 12, 1559: 1-16.

[78] Ranby B.G. The mercerization of cellulose. Acta Chem. Scand., 1952; 6: 101-115.

[79] Osovskaya I., Dimarchuck N., Mishenko K. Thermochemical study of interaction of cotton cellulose with water and aqueous solutions of sodium hydroxide. J. Appl. Chem., 1971; 44: 2525-2528.

[80] Ioelovich M. Peculiarity of phase transitions of cellulose nanocrystallites. ChemXpress. 2016; 9: 1-14.

[81] Agarwal U.P., Ralph S.A., Baez C., et al. Detection and quantitation of cellulose II by Raman spectroscopy. Cellulose, 2021; 28: 9069–9079.

[82] Fengel D., Jakob H., Strobel C. Influence of the alkali concentration on the formation of Cellulose II. Holzforschung, 1995; 49: 505-511.

[83] Nishiyama Y., Kuga Sh., Okano T. Mechanism of mercerization revealed by X-ray diffraction. J. Wood Sci., 2000; 46: 452-457.

[84] Yokota H., Sei T., Horii F., Kitamaru R. ^{13}C CP/MAS NMR study on alkali cellulose. J. Appl. Polym. Sci., 1990; 41: 783-791.

[85] Karasev N., Dimarchuck N., Mishenko K. On interaction mechanism of cellulose with aqueous solutions of sodium hydroxide. J. Appl. Chem., 1967; 40: 1573- 1579.

[86] Ioelovich M. Thermochemistry of alkalization and etherification of cellulose. WJARR, 2023; 20: 1166–1174.

[87] Dasoyan M. Starter batteries: the device, operation, and maintenance. Trans: M.; 1991.

[88] Ioelovich M. Adjustment of hydrophobic properties of cellulose materials. Polymers, 2021; 13: 1-12.

[89] Wei DW, Wei H, Gauthier AC, et al. H. Superhydrophobic modification of cellulose and cotton textiles: Methodologies and applications. J. Biores. Bioprod. 2020; 5: 1–15.

[90] Gocho H, Shimizu H, Tanioka A, et al., 2000. Effect of acetyl content on the sorption isotherm of water by cellulose acetate: comparison with the thermal analysis results. Carbohydrate Polym. 2000; 41: 83-86.

[91] Ioelovich M. Study of water vapor sorption by cellulose esters with different degrees of substitution. WJARR, 2922; 15: 214-222.

[92] Edgar KJ, Buchanan CM, Debenham JS, et al. Advances in cellulose ester performance and application. Progress in Polym. Sci. 2001; 26: 1605-1688.

[93] Okamura K, Norimoto M, Shiraishi N. Chance od X-diffraction peaks in aliphatic cellulose esters homologues. Wood Res. 1983; 69: 89-90.

[94] Crépy L, Miri V, Joly N, et al. Effect of side chain length on structure and thermomechanical properties of fully substituted cellulose fatty esters. Carbohydr. Polym. 2011; 83: 1812-1820.

[95] Willberg-Keyrilainen P, Ropponen J. Evaluation of esterification routes for long chain cellulose esters. Helyon, 2019; 5: 1-6.

[96] Ioelovich M. Application of thermochemical methods for the study of cellulose and cellulose esters. WJARR, 2023; 18: 1477–1488.

[97] Ioelovich M. Thermodynamics of cellulose esterification. WJARR, 2023; 19: 225–232.

[98] Ioelovich M. Thermodynamic analysis of cellulose nitration. WJARR, 2024; 21: 485–494.

[99] Mattar H, Baz Z, Saleh A, et al. Nitrocellulose: structure, synthesis, characterization, and applications. Water, Energy, Food and Env. J. 2020; 1: 1-15.

[100] Cheung C. Studies of the Nitration of Cellulose – Application in New Membrane Material. Diss. Thesis. Vancouver; 2014.

[101] Trache D, Khimeche K, Mezroua A, Benziane M. Physicochemical properties of microcrystalline nitrocellulose from alpha grass fibers and its thermal stability. J. Therm. Anal. Calorim. 2016; 124:1485–1496.

[102] Obolenskaya AV, Elnitskaya ZP, Leonovich AA. Laboratory Practicum on Chemistry of Wood and Cellulose. Ecology; 1991.

[103] Cheung C. Studies of the Nitration of Cellulose – Application in New Membrane Material. Diss. Thesis. Vancouver; 2014.

[104] Panchenko O, Tutova O. Problems and advances in production of nitrate cellulose. Chem. Plant Mater. 2005; 3: 85–88.

[105] Ioelovich M. Study of heat effects of topochemical esterification of cellulose. WJARR, 2024; 23: 1232–1241.

[106] Larina VN, Uryash VF, Kushch DS. Thermochemical characteristics of cellulose acetates with different degrees of substitution. J. Phys. Chem. 2012; 86: 1776–1778.

[107] Stovbun SV, Nikolskiy SN, Melnikov VP, et al. Chemical physics of cellulose nitration. J. Phys. Chem. 2016; 10: 245–259.

[108] Ioelovich M, Saini S, Sharma T, Singh B. Cellulose-Based NanoBioMaterials. Ch.11. In: Emerging Trends in NanoBioMedicine. Editors: B. Singh, O.P. Katare, and E.B. Souto. CRC Press: Boca Raton; 2019.

[109] Duceac IA, Tanasa F, Coseri S. Selective oxidation of cellulose - a multitask platform with significant environmental impact. Materials, 2022; 15: 1-25.

[110] Sultana N, Edlund U, Guria C, Westman G. Kinetics of Periodate-Mediated Oxidation of Cellulose. Polymers, 2024; 16: 381.

[111] Vozniuk ON, Blinov IA, Laskin BM, et al. Optimization of oxidation of cellulose by dinitrogen tetraoxide for industrial application. J. Chem. Technol. Metallurgy. 2022; 57: 1142-1150.

[112] Sinha TJ, Vasudevan P. Blood-cellulosic interactions. Biomater. Med. Devices Artific. Organs. 1984; 12: 273-87.

[113] Lochman P, Plodr M, Páral J, Šmejkal K. Nanofiber micro-dispersed oxidized cellulose as a carrier for topical antimicrobials: first experience. Surgical Infections. 2010; 11: 29-32.

[114] Gensh KV, Bazarnova NG. Oxidized cellulose in medicine. Chem. Plant Materials. 2013; 4: 13-20